

***Mathematical Modeling and Finite Element Simulation of Fatigue Failure of  
Boiler Heat Tube***



**JIMMA UNIVERSITY  
SCHOOL OF GRADUATE STUDIES  
JIMMA INSTITUTE OF TECHNOLOGY  
FACULTY OF MECHANICAL ENGINEERING  
MANUFACTURING SYSTEMS ENGINEERING STREAM**

A Thesis Submitted to Graduate Studies of Jimma University in Partial Fulfillment of the Requirements for the Degree of Master Science in Mechanical Engineering (Manufacturing Systems Engineering).

**By: TAMIRU HAILU KORI**

**Feb 2020  
JIMMA, ETHIOPIA**

**JIMMA UNIVERSITY**  
**SCHOOL OF GRADUATE STUDIES**  
**JIMMA INSTITUTE OF TECHNOLOGY**  
**FACULTY OF MECHANICAL ENGINEERING**  
**MANUFACTURING SYSTEMS ENGINEERING STREAM**

*Mathematical Modeling and Finite Element Simulation of Fatigue Failure of Boiler Heat  
Tube*

A Thesis Submitted to Graduate Studies of Jimma University in Partial Fulfillment of the  
Requirements for the Degree of Master Science in Mechanical Engineering (Manufacturing  
Systems Engineering).

**By: TAMIRU HAILU KORI**

**ID No. RM0287/10**

Main Advisor: Dr. Mesay Alemu (Ass. Prof.)

Co-Advisor: Mr. Wondimu Fanta (M.Sc.)

**Feb 2020**  
**JIMMA, ETHIOPIA**

**JIMMA UNIVERSITY**  
**JIMMA INSTITUTE OF TECHNOLOGY**  
**POSTGRADUATE PROGRAM**

This is to certify that the thesis prepared by Tamiru Hailu Kori, entitled: *“Mathematical Modeling and Finite Element Simulation of Fatigue Failure of Boiler Heat Tube”* and submitted in partial fulfillment of the requirements for the degree of masters of Science in Mechanical Engineering (Manufacturing Systems Engineering) complies with the regulations of the university and meets the accepted standards with respect to the originality and quality.

Approved by the Examining Committee:

|                            |  |                   |
|----------------------------|--|-------------------|
| _____                      | _____  | _____             |
| Advisor                    | Signature  | Date              |
| <b>Dr. Moera Gutu Jiru</b> |  | <b>05/03/2020</b> |
| External Examiner          | Signature  | Date              |
| _____                      | _____  | _____             |
| Internal Examiner          | Signature  | Date              |
| _____                      | _____  | _____             |
| Chairman                   | Signature  | Date              |

## Declaration

I hereby declare that the research work entitled modeling the *Mathematical Modeling and Finite Element Simulation of Fatigue Failure of Boiler Heat Tube*. This research is my original work and has not been presented for a degree in any other university.

Name: - Tamiru Hailu

---

Signature

---

Date

This research submitted for examination with my approval as university supervisor.

Name: - Dr. Mesay Alemu

---

Advisor

---

Date

Name: - Mr. Wendimu Fanta

---

Co-Advisor

---

Date

Name: - Kancharla Srinivasarao

---

Chairman

---

Date

## **Acknowledgment**

I would first like to thank my advisor Dr. Mesay Alemu who consistently guide me in the right direction whenever he thought I needed it and whenever I run to a trouble spot or had a question about my research or writing.

I would also like to acknowledge my co-advisor Mr. Wendimu Fanta who guide and gave me very valuable comments on this thesis.

I would like to thank lastly the friends and colleagues who has given advice, motivation and inspiration during this work. And also I would have special gratitude to Faculty Mechanical Engineering which facilitates necessary requirements during this study.

## **Abstract**

*Boiler heat tube is the main component of power plant where the water is changed to high-pressure steam, it operates under corrosive environment and high temperature. This corrosive environment and cyclic temperature fluctuation cause corrosion fatigue on boiler heater tube, and which degrade life of the component. Fatigue in corrosive environment is a situation where there is premature failure due to the action of corrosion at the surface, which shortens the time required for the crack initiation. The rate of corrosion can be affected by factors like temperature, pressure and presence of moisture that increase the rate of chemical reaction.*

*This thesis presents corrosion rate by volumetric pit growth, crack initiation and crack propagation of boiler heat tube for power plant under cyclic thermal load. 8.72Cr-0.9Mo steel is one of the steel type which mostly used nowadays as boiler heat tube. Volumetric pit growth rate used for crack initiation and energy release rate approach (J-integral) used to find crack propagation. Temperature taken in the interval of 25°C-500°C, and it has a significant effect on rate of reaction and material properties. The results shows 906Mpa and 895Mpa thermal stress induced at crack tip at 500°C from analytical and FEM respectively. And also energy release rate results are 33.4J/mm<sup>2</sup> and 35.43N/mm<sup>2</sup> from analytical and FEM respectively. The result shows the material reach fatigue limit in the range of low cycle fatigue having the value less than 10<sup>4</sup> cycles. The existence of corrosion reduce crack initiation cycles since crack initiation is speed up by the presence of corrosion pit. The results from both analytical approach and FEM have a good agreement with other literatures.*

**Keywords:** *Corrosion, corrosion pit, crack initiation, crack propagation, strain energy release rate, strain energy density.*

## **Acronyms**

|      |  |
|------|--|
| ASTM | American Society for Testing and Materials |
| ASME | American Society of Mechanical Engineering |
| CAE  | Complete ABAQUS environment                |
| CR   | Corrosion rate of carbon steel             |
| CFC  | Corrosion fatigue cracking                 |
| SCC  | Stress corrosion cracking                  |
| CTOD | Crack tip opening displacement             |
| FEM  | Finite element method                      |
| FGM  | Functionally graded material               |
| HCF  | High cycle fatigue                         |
| LCF  | Low cycle fatigue                          |
| SIF  | Stress intensity factor                    |

## Nomenclature

|                 |   |
|-----------------|---|
| a               | Crack depth size (mm)                                 |
| $a_{cr}$        | Critical crack length (mm)                            |
| c               | Crack opening radius (mm)                             |
| C               | Material constant ranges between (1.002 to 1.02)      |
| $C_p$           | Volumetric pit growth rate ( $m^3/s$ )                |
| E               | Young's modulus of the material (Gpa)                 |
| $E\alpha$       | Activation energy (KJ/mol)                            |
| F               | Faraday's constant (C/Kg-mol)                         |
| $I_o$           | Pitting current ( $\mu m/cm^2$ )                      |
| $K_{IC}$        | Fracture toughness (Mpa $\sqrt{m}$ )                  |
| n               | Number of valance                                     |
| $N_i$           | Number of cycles crack initiation (Cycle)             |
| $N_p$           | Number of cycles crack propagation to failure (Cycle) |
| R               | Gas constant (J/mol.K)                                |
| T               | Temperature (K)                                       |
| $\Delta T$      | Change in temperature (K)                             |
| t               | Time (s)  |
| $\sigma_y$      | Yield strength (Mpa)                                  |
| v               | Poison's ratio  |
| $\sigma_a$      | Axial stress or longitudinal stress (Mpa)             |
| $\sigma_\theta$ | Circumferential stress or hoop stress (Mpa)           |



## Nomenclature

|                      |   |
|----------------------|---|
| $\sigma_r$           | Radial stress (Mpa)                               |
| $\varepsilon_a$      | Axial strain                                      |
| $\varepsilon_\theta$ | Circumferential strain                            |
| $\varepsilon_r$      | Radial strain                                     |
| $\Delta\varepsilon$  | Cyclic strain range                               |
| $\rho$               | Density (Kg/m <sup>3</sup> )                      |
| $\alpha$             | Thermal expansion coefficient (K <sup>-1</sup> )  |
| $\Delta K$           | Stress intensity factor (Mpa√m)                   |
| $\Delta\sigma$       | Stress range (Mpa)                                |
| Q                    | Geometric correction factor                       |
| c                    | Fatigue ductility exponent                        |
| $\varepsilon'_f$     | Fatigue ductility coefficient                     |
| w                    | Plastic strain energy density (J/m <sup>3</sup> ) |
| $\Delta J$           | Cyclic j-integral (J/m <sup>2</sup> )             |

# Table of Contents

|  |     |
|--|-----|
| Declaration .....                        | I   |
| Acknowledgment .....                     | II  |
| Abstract .....                           | III |
| Acronyms .....                           | IV  |
| Nomenclature .....                       | V   |
| Table of Contents .....                  | VII |
| List of Tables .....                     | X   |
| List of Figures .....                    | XI  |
| Chapter One .....                        | 1   |
| 1 Introduction.....                      | 1   |
| 1.1 Background.....                      | 1   |
| 1.2 Motivation.....                      | 3   |
| 1.3 Factors Affecting Fatigue life ..... | 5   |
| 1.3.1 Environment.....                   | 5   |
| 1.3.2 Stress Ratio .....                 | 6   |
| 1.3.3 Stress Intensity.....              | 7   |
| 1.3.4 Types of Load .....                | 7   |
| 1.3.5 Fracture Toughness.....            | 7   |
| 1.4 Structure of the Thesis .....        | 7   |
| 1.5 Scope of the Study .....             | 8   |
| 1.6 Significance of the Study .....      | 8   |
| 1.7 Statement of the Problem.....        | 8   |
| 1.8 Objectives of the Thesis.....        | 9   |
| 1.8.1 Main objective .....               | 9   |
| 1.8.2 Specific objectives .....          | 9   |
| Chapter Two.....                         | 10  |
| 2 Literature Review.....                 | 10  |
| 2.1 Introduction.....                    | 10  |
| 2.2 Review on Crack Initiation .....     | 11  |

|  |    |
|--|----|
| 2.3 Review on Crack Propagation .....  | 13 |
| 2.4 Research Gap .....   | 14 |
| Chapter Three.....   | 16 |
| 3 Research Methodology .....   | 16 |
| 3.1 Introduction.....  | 16 |
| 3.2 Selection of Appropriate Approach .....  | 17 |
| 3.2 Tools or Techniques.....   | 17 |
| 3.3 Data Processing, Analysis and Interpretation Techniques.....                     | 17 |
| 3.4 Materials .....  | 18 |
| Chapter Four .....   | 19 |
| 4 Analytical modeling and finite element simulation .....                            | 19 |
| 4.1 Introduction.....  | 19 |
| 4.2 Analytical approach .....  | 20 |
| 4.2.1 Basic Assumptions.....   | 20 |
| 4.2.2 Temperature-Dependent Material properties.....                                 | 21 |
| 4.2.3 Thermal Stress (Circumferential and Longitudinal Stress) .....                 | 22 |
| 4.2.4 Temperature distribution through thickness .....                               | 23 |
| 4.2.5 Thermal Strain .....   | 24 |
| 4.2.6 Load Cycles .....  | 25 |
| 4.2.7 Low Cyclic fatigue.....  | 26 |
| 4.2.8 Modes of Failure .....   | 28 |
| 4.3 Crack Initiation .....   | 29 |
| 4.3.1 Corrosion Rate .....   | 29 |
| 4.3.2 Effect of Temperature on Corrosion .....                                       | 31 |
| 4.3.3 Pitting.....   | 32 |
| 4.3.4 Pit to Crack Transition.....   | 33 |
| 4.4 Crack Propagation.....   | 38 |
| 4.4.1 Prediction of Strain based fatigue life using Manson and Coffin Equation ..... | 38 |
| 4.4.2 J-Integral Approach for Large Plastic Strain .....                             | 42 |
| 4.5 Finite Element Method Simulation.....  | 43 |
| 4.5.1 Procedures.....  | 44 |

|   |    |
|---|----|
| 4.5.2 Creating Part in ABAQUS.....              | 45 |
| 4.5.3 Mesh Type .....                           | 46 |
| 4.5.4 Simulation Result.....                    | 47 |
| Chapter Five.....                               | 49 |
| 5 Results and Discussion .....                  | 49 |
| Chapter Six.....                                | 56 |
| 6 Conclusion and Recommendation .....           | 56 |
| 6.1 Conclusion .....                            | 56 |
| 6.2 Recommendation .....                        | 58 |
| References.....                                 | 59 |
| Appendixes .....                                | 63 |
| Appendix A.....                                 | 63 |
| Table A-1 .....                                 | 63 |
| Table A-2 .....                                 | 64 |
| Appendix B.....                                 | 65 |
| Tubes Wall Thickness and Outside Diameter.....  | 65 |
| Appendix C.....                                 | 67 |
| Analytical approach additional calculation..... | 67 |

## List of Tables

### Chapter Three

Table 3. 1 Chemical Composition of 8.72Cr-0.9Mo steel..... 18

Table 3. 2 Mechanical Properties of 8.72Cr-0.9Mo steel..... 18

### Chapter Four

Table 4. 1 Cyclic ductility exponent and cyclic ductility coefficient at different temperature of 8.72Cr-0.9Mo steel ..... 39

# List of Figures

## Chapter One

|   |   |
|---|---|
| Figure 1. 1 Corrosion of boiler tube and its failure.....                   | 4 |
| Figure 1. 2 Fire tube boiler and water tube boiler.....                     | 4 |
| Figure 1. 3 Schematic diagram of steam power plant.....                     | 5 |
| Figure 1. 4 Cracking. Transgranular (a) and intergranular cracking (b)..... | 6 |

## Chapter Three

|   |    |
|---|----|
| Figure 3. 1 Flow diagram of research methods..... | 16 |
|---|----|

## Chapter Four

|  |    |
|--|----|
| Figure 4. 1 Young's modulus response to change in temperature .....  | 21 |
| Figure 4. 2 Response of stress to temperature change .....   | 23 |
| Figure 4. 3 Stress induced on outer surface of heat tube .....   | 23 |
| Figure 4. 4 Response of thermal strain to change in temperature.....   | 25 |
| Figure 4.5 Sinusoidal load cycles .....  | 25 |
| Figure 4. 6 Cyclic load. (a) load with both $\sigma_{max}$ and $\sigma_{min}$ positive (b) load with $\sigma_{max}$ and $\sigma_{min}$ zero..... | 26 |
| Figure 4. 7 A schematic of typical S-N curve showing the stress amplitude versus cycles to failure .....   | 27 |
| Figure 4. 8 Opening or mode I (left), sliding or mode II (middle) and tearing or mode III (right) .....  | 28 |
| Figure 4. 9 Anodic and cathodic reaction the metal under corrosion .....   | 30 |
| Figure 4. 10 Change of corrosion rate with temperature .....   | 32 |
| Figure 4. 11 Pit formation.....  | 33 |
| Figure 4. 12 Elliptical pit opening and its depth or length.....   | 34 |
| Figure 4. 13 Volumetric pit growth rate at different temperature.....  | 35 |
| Figure 4. 14 Change of stress intensity factor and pit size at different cyclic stress .....   | 36 |
| Figure 4. 15 Plastic zone for semi-ellipsoidal crack.....  | 37 |
| Figure 4. 16 Number of cycles to initiate crack.....   | 38 |
| Figure 4. 17 Plot of cyclic ductility exponent and cyclic ductility coefficient at different temperature of 8.72Cr-0.9Mo steel.....              | 40 |

|   |    |
|---|----|
| Figure 4. 18 Response of the 9Cr-1Mo steel to temperature in number of cycles .....         | 40 |
| Figure 4. 19 Effect of crack size on number of cycles.....                                  | 41 |
| Figure 4. 20 Strain amplitude versus number of reversal to failure.....                     | 41 |
| Figure 4. 21 Crack propagation rate versus cyclic J-integral using analytical approach..... | 43 |
| Figure 4. 22 Flow chart shows the procedure in finite element method.....                   | 45 |
| Figure 4. 23 Abaqus model of boiler heater tube.....  | 46 |
| Figure 4. 24 Triangular mesh surface of the tube .....                                      | 46 |
| Figure 4. 25 Stress distribution around crack tip (Von-Mises stress).....                   | 47 |
| Figure 4. 26 Strain at the crack tip under thermal stress.....                              | 48 |
| Figure 4. 27 Plastic strain energy density (PENER).....                                     | 48 |

## **Chapter Five**

|   |    |
|---|----|
| Figure 5. 1 Volumetric pit growth rate response to temperature change.....  | 50 |
| Figure 5.2 Comparison between analytical, FEM and experimental result using strain amplitude versus number of reversal to failure at 500°C..... | 51 |
| Figure 5. 3 Comparison between fatigue with corrosion pit and without corrosion pit .....   | 52 |
| Figure 5. 4 Comparison of analytical, FEM and experimental data of crack growth rate versus cyclic J-integral.....                              | 53 |
| Figure 5. 5 Comparison between analytical, FEM and other literature, crack initiation and crack propagation results .....                       | 54 |

# Chapter

# 1

## Introduction

### 1.1 Background

Failure is a problem that society has faced for as long as there have been man-made structures. The engineering communities have responded to prevent failure occurring. The discovery of fatigue occurred in the 1800s when several investigators in Europe observed that bridge and railroad components cracking when subjected to repeated loading [1]. In 20 century, many revolutionary design philosophies, inspection techniques and practices, material development and material processing and controls have redefined the criteria for failure. During the past four decades, an extensive research of fracture mechanics has greatly enhanced the understanding of structural failure [1]. Today, fracture mechanics is not only of academic interest and also plays an increasingly important role in structural design.

Fatigue is the failure of material caused by cyclic loading. It is the most common source of behind failures of mechanical and thermal loaded structures. The process until a component finally fails under repeated loading can be divided into three stages. The first stage is during large number of cycles, the damage develops on the microscopic level and grows until a macroscopic crack is formed (initiation stage). The second is macroscopic crack grows for each cycles until it reaches a critical length (propagation stage). And the third stage is cracked component breaks because it can no longer sustain the peak load.

This kind of fatigue is one of the forms of environmentally induced cracking. Fatigue will be enhanced by an increased chemical activity of the environment. Some of the factors that have a strong influence on corrosion fatigue are temperature, PH, pressure of the gaseous environment, and concentration of the corrosion species [7]. It is an important but complex



mode of failure for high-performance structural metals operating in deleterious environments [8].

Corrosion of metals is an electrochemical reaction that involves changes in both the metal and the environment in contact with the metal. It is a dangerous and extremely costly problem. Fatigue in corrosive environment is defined as the sequential stages of metal damage that evolve with accumulated load cycling, in an aggressive environment compared to inert or benign surroundings, and resulting from the interaction of irreversible cyclic plastic deformation with localized chemical or electrochemical reactions.

And also corrosion fatigue can be defined as the phenomenon of cracking in materials under the combined action of fatigue (or cyclic) loading and a corrosive (or deleterious) environment (gaseous or aqueous). This phenomenon is occur in many engineering alloys over a broad range of environments and has been recognized as an important cause of failure of engineering structures [9].

Fatigue in corrosive environment does not occur unless the material is susceptible to stress corrosion cracking (SCC) in particular environment, so corrosion fatigue is always a subject of stress corrosion cracking. SCC is the result of stress concentration at corrosion generated surface flaws (as quantified by the stress-intensity factor) and this flaw surface growth to pit under the action of chemical and thermal influence. Before crack propagation pit will grow to critical size, where the pit changed to crack. Pre corrosion followed by loading in an inert environment will not result in any significant crack propagation, while simultaneous environmental exposure and application of stress will cause time-dependent subcritical crack propagation [9]. Due to stress intensity at flawed surface crack nucleation/initiation begins.

Corrosion affects the strength of the metals and due to that, the life is degraded under cyclic operation. The degradation in service life is a function operating environment. For the boiler heat tube which is operated under high-temperature steam the rate of corrosion adversely increased. The fatigue life of the boiler heat tube is a combined effects of thermal stress that create stress on tube and corrosion.

Fatigue is greatly reduce the duty life of the boiler heat tube. Comparison between the fatigue without corrosion and fatigue with corrosion which has a significant drop in strength of the metals. One of the main differences between corrosion fatigue and inert-environment fatigue is that there is no “safe stress range” at which metal has infinite life. ASTM 8.72Cr-0.9Mo steel (T91) steel is used in a very aggressive environment and where it is subjected to thermal cyclic loading. In boiler, the heat tube subjected to high thermal stress rather than mechanical stress.

Corrosion is a type of chemical change. It results in the formation of Iron Oxide which is an entirely new substance. The corrosion results significant effects on the service life of materials especially metals. And also the rate of corrosion is depends on the environment.

## **1.2 Motivation**

Boiler tube is one of the main components of power generation system in power plant where water is changed to high-pressure steam to drive the turbine. Failure of this part cause failure of the whole system. This failure can be caused by different mechanisms, corrosion is the main cause pitting of surface of tube which later changed to crack under the action of cyclic thermal loading. This failure has a complex phenomenon however, corrosion pits caused crack accounts more for failure of this component. Crack is propagated by cyclic thermal loading, which results from large plastic deformation at the crack tip.

There are many factors corrosion to occur; the factors like presence of moisture, surface irregularity, presence of oxygen and inhibitors. Temperature is a parameter which accelerate the rate of corrosion.

Since the outer surface of the tube exposed to corrosive environment, corrosion occurred or detected on the surface. The localized corrosion attack on the surface of the tube create a pit and under cyclic thermal stress this pit grow to crack or initiate a crack. Thermal stress cycles happened during heating and cooling of the system. The cycles is natural in power plant since there is cyclic operation and shutdown cycles.

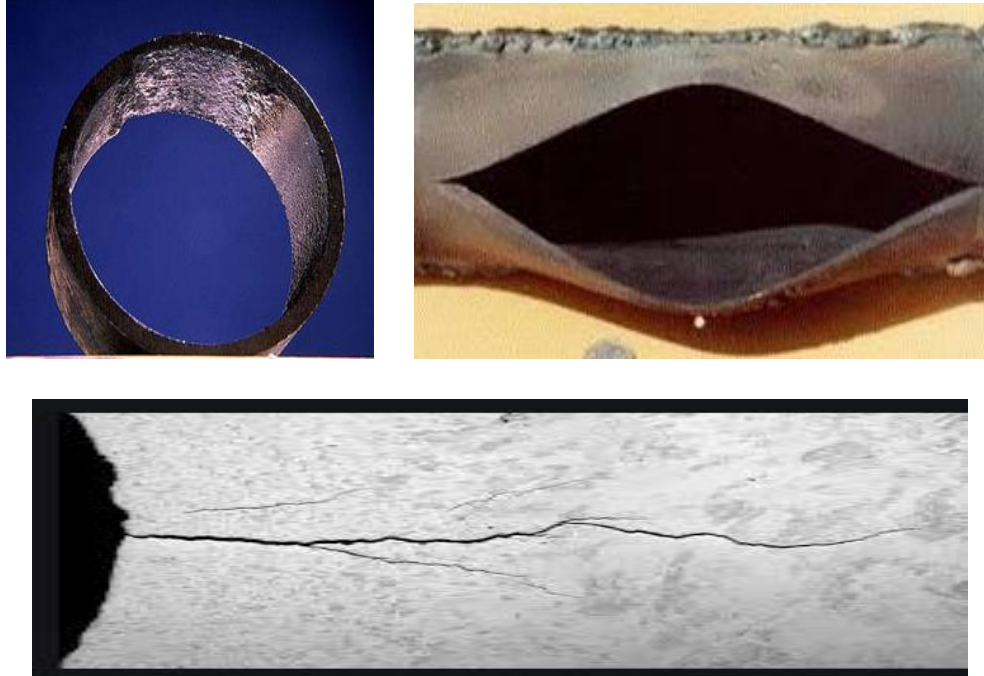


Figure 1. 1 Corrosion of boiler tube and its failure [19]

The figure below illustrates the main components of power generation system, externally fired type boiler tube. Thermal energy generated from combustion of coal, petroleum, nuclear, geothermal, solar thermal electric, waste incineration as well as natural gas. Heat is generated by burning a fossil fuel; the combustion gas can be ducted around tubes containing the water (water-tube boiler), or the hot gas can pass inside the tubes with the water being in the shell (fire-tube boiler).

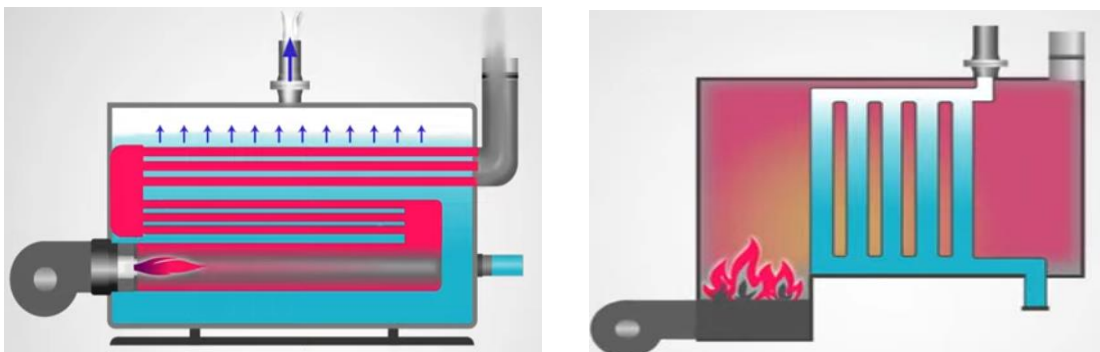


Figure 1. 2 Fire tube boiler and water tube boiler

Fire tube boiler or heat tube is focus of this study. Figure (1.3) shows schematic diagram of the whole steam power plant systems.

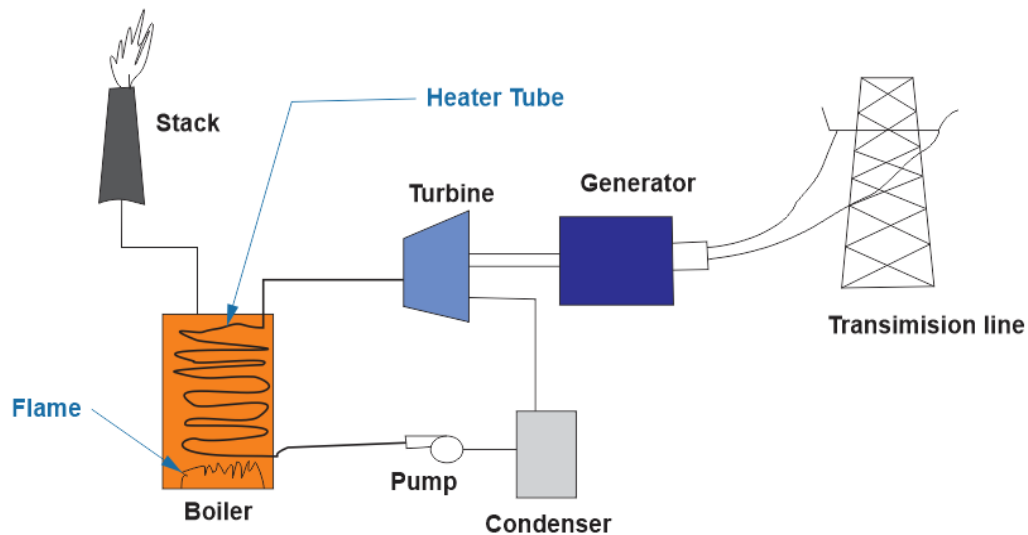


Figure 1. 3 Schematic diagram of steam power plant

### 1.3 Factors Affecting Fatigue life

In material science, fatigue is the weakening of the material caused by cyclic loading that results in progressive and localized structural damage and the growth of crack. Crack initiation and crack propagation are two separate processes driven by different phenomenon. It is then important to notice that the corrosion media will have a different effect on each of them. Fatigue life is influenced by a variety of factors, such as temperature, surface finish, metallurgical microstructure, presence of oxidizing or inert chemicals, residual stresses, scuffing contact (fretting), etc. The factors that affect the fatigue life are discussed as follow:

#### 1.3.1 Environment

Corrosion will be enhanced by an increased chemical activity of the environment. Some factors that have a strong influence on corrosion rate are temperature, PH, pressure of gaseous environment and concentration of the corrosion species.

##### 1. Temperature

Temperature may influence the environment or metal surface reactions as well as many transport processes involved in corrosion, temperature can be affect corrosion pit growth rates.

Temperature do not only affect the rate of corrosion but also the properties of materials (mechanical properties) like yield strength, tensile strength, Young modulus, etc. Those parameters are temperature-dependent parameters which results change in fatigue life of material under cyclic loading. Fatigue crack growth rates increase with increasing temperature. At surface, crack grew mainly intergranular but can be transform to transgranular cracks when propagated into bulk. At higher temperature, crack initiation can be either transgranular or intergranular.

Intergranular fracture is type of fracture in which the crack propagate along the grain boundaries of the material. In transgranular crack grows through the material grains rather than at grain boundaries.

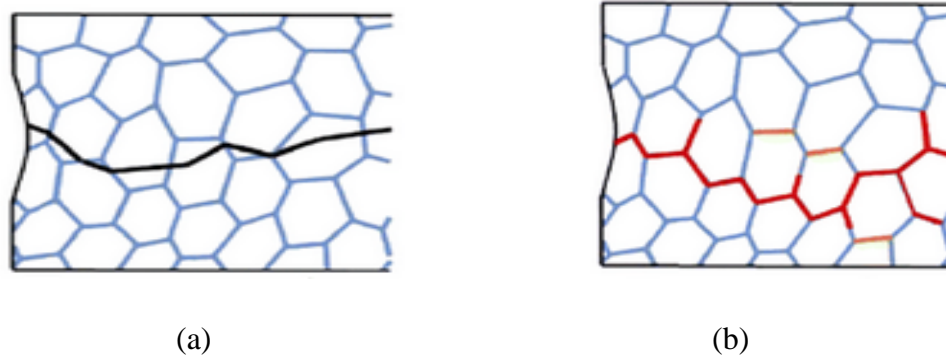


Figure 1. 4 Cracking. Transgranular (a) and intergranular cracking (b) [40]

## 2. Moisture

Moisture affect the chemical and mechanical processes of decay. On a surface with moisture, particles have a better possibility of adhering and water-soluble gases are more readily captured. Both gas and particle fluxes increase when condensation takes place on the material surface. This water-soluble gases increase the rate of corrosion of the material and it increase the rate of pit growth which is later changed to crack under cyclic loading.

### 1.3.2 Stress Ratio

When stress is positive the crack will open, leaving the fresh material in its interior exposed to aggressive atmosphere. The longer the time of exposure, the higher the corrosion damaged suffered at the crack tip. The rate of crack propagation are increased by high-stress ratios. If

stress ratio is increased while the stress intensity ( $\Delta K$ ) is held constant, the crack tip strain and strain rate are increased, therefore crack propagation increased.

### **1.3.3 Stress Intensity**

Although the correlation between the stress intensity and corrosion fatigue cracking varies noticeably. The general tendency is that crack growth rates in corrosion fatigue increase when increasing the stress intensity.

### **1.3.4 Types of Load**

Load type significantly affect fatigue life of the material under cyclic loading. A load might be tensile, compressive or shear and these loads are different effect on fatigue life. Tensile load is significant for mode I cracking type, but compressive load reduce the effect of cracking, even it compressive residual stress added to material to resist failure under tensile load. Shearing load is significant in mode II cracking type which occurs by shearing along the plane.

### **1.3.5 Fracture Toughness**

Fracture toughness is an indication of the amount of stress required to propagate a preexisting flaw. The fracture toughness of a metal depends on the following factors:

1. Metal composition
2. Metal temperature
3. Extent of deformation to the crystal structure
4. Metal grain size
5. Metal crystalline form

## **1.4 Structure of the Thesis**

This thesis have the following structure:

- In chapter one, introductory part of the thesis have discussed, fatigue life under corrosive environment and thermal stress are briefly discussed. Then also objectives of the research are also discussed in the first chapter.
- The literature review is summarized in the second chapter.
- In chapter three methods used during this study have included.
- Analytical modeling and software simulation are discussed in detail in fourth chapter.
- Results and discussion are in fifth chapter.

- Finally, conclusion and recommendation for further work are mentioned in last chapter.

## **1.5 Scope of the Study**

The scope of this research thesis is modeling of fatigue failure for boiler heater tube in thermal (steam) power plant. Considering the parameters: corrosion as a function of temperature, thermal stress and non-linearity of the material with change in temperature. Mainly it focusing on pit growth rate, pit to crack transition, crack propagation and predicting total fatigue life of boiler heater tube in power plant. The study limited to only fatigue life, not include failure induced by creep. Since the operating temperature of boiler donot exceed half of the melting temperature of the selected steel type. Below this temperature creep do not initiate.

## **1.6 Significance of the Study**

Steam power plants lose billions of dollar due to fatigue annually, especially fatigue initiated by corrosion. The significance of this research is study the parameters that are very significant for initiation and propagation of this kind of fatigue. One should know for how much time the part can serve before failure happens, by knowing the rate of corrosion or pit growth rate, crack growth rate and fatigue life prediction. Generally, this research will have the following significance:

- Estimating the number of cycles to initiate the crack by finding the volumetric pit growth rate.
- Calculating crack propagation rate and fatigue life in both analytical and finite element method (FEM) approach.
- It helps to utilize energy and energy efficiently, taking immediate action before failure happens and maintaining the part before failure by knowing the above-listed points.
- It eliminate a guesswork by making decision depending on scientific methods knowing exact life (service life) and replacing the part.

## **1.7 Statement of the Problem**

In the steam power plant corrosion pit induced crack is the main cause of the failure of boiler heater tube. Corrosive environment and high temperature which the boiler operate in, are greatly increase this failure rate and it makes the overall power generation out of service.

Corrosion that cause crack nucleation or crack initiation due to thermal stresses (stress intensity) at flaw surface of the heater tube caused by corrosion was not studied; specifically for boiler heat tube in power plant for 8.72Cr-0.9Mo steel material, which now day boiler tube made of it. The model described the condition of the system in good manner by taking fatigue life into two separate stage. In-pit to crack transition stage stress intensity factor-based approach and volumetric pit growth rate used and then j-integral approach used in crack propagation period. Taking those conditions into consideration the fatigue mechanism can appropriately described. In general, this research addressed the fatigue life under corrosion and thermal stress, and predicted the fatigue life of the boiler heat tube.

## **1.8 Objectives of the Thesis**

### **1.8.1 Main objective**

The main objective of this thesis is mathematical modeling and simulation of fatigue failure using software for boiler heat tube under corrosive environment and thermal stress.

### **1.8.2 Specific objectives**

The specific objectives includes the following

- Deriving the expression of volumetric corrosion pit growth rate as a function of temperature and analytically calculating pit growth rate.
- Finding pit to crack transition cycle life under cyclic thermal stress by taking the critical value at which pit is transited to crack.
- Estimation of crack propagation rate in plastic deformation at crack tip in strain-based approach.



## Chapter



## Literature Review

### 2.1 Introduction

Fatigue refers to a type of engineering failure in which the material tends to fracture by crack formation under the application of repeated cyclic stress or load. The material fractures by fatigue in three steps, initiation of crack, crack growth and propagation and finally the material fails. There are many factors to initiate crack and speed up crack propagation rate. These factors are porous during manufacturing, corrosion pitting, wear generated under operation of the component and etc.

Thermal fatigue is a fatigue failure with macroscopic cracks resulting from cyclic thermal stresses and strains due to temperature changes, spatial temperature gradients, and high temperatures under constrained thermal deformation [4]. Thermal fatigue may occur without mechanical loads. The combination of corrosion pitting and thermal stress significantly reduce fatigue failure life of the components.

Corrosion is a natural process that converts a refined metal into a more chemically-stable form such as oxide, hydroxide, or sulfide. It is the gradual destruction of materials (usually a metal) by chemical and/or electrochemical reaction with their environment. The more conventional explanation for pitting corrosion is that it is an autocatalytic process. Metal oxidation results in localized acidity that is maintained by the spatial separation of the cathodic and anodic half-reactions, which creates a potential gradient and electromigration of aggressive anions into the pit [3].

The corrosion of materials is often a life-limiting process that affects almost all materials. A single pit in a critical point can cause a great deal of damage. As it was mentioned in the previous part corrosion fatigue is lead to the failure of the whole power plant since the boiler heat tube is one of the main and very important component. The damage is often manifested as accelerated fatigue crack nucleation and/or propagation. There are many researches have conducted around this area. High temperatures and stresses in the boiler metal tend to accelerate the corrosive mechanisms. In the steam and condensate system corrosion is generally the result of contamination with carbon dioxide and oxygen.

## **2.2 Review on Crack Initiation**

Cyclic stresses are created by rapid heating and cooling and are concentrated at points where corrosion has roughened or pitted the metal surface. Fatigue crack initiation behavior of low-alloy steel in 90 C deionized water was investigated by Kondo Y. and tried to observe three corrosion fatigue processes pit growth, crack formation and crack propagation [6]. And also Richard P. studied corrosion fatigue damage accumulates with increasing load cycle count (N) and in four stages: cyclic plastic deformation, microcrack initiation, small crack growth to linkup and coalescence, and macro crack propagation [8].

According to Tu S.et.al. fatigue is a cascade of processes of crack formation and growth that depends on the several factors like: microstructural features, loading condition and distribution of localized cyclic plastic deformation [2]. For example, cracks may form at matrix–inclusion interfaces, assisted by matrix strain localization associated with interfacial debonding or particle fracture. Crack initiation, and the whole fatigue process, is controlled by cyclic plastic deformation. They have focused initiation at persistent slip band, initiation at grain boundraies, effects of surface treatement and also observed models for crack initiation at surface level and sub surface level.

Cracking of the boiler tube had occurred by thermal fatigue. Casey T. et.al. experimetyly investigated the difference in thermal heating/expansion of the water-filled boiler tube had applied high thermal strains onto the tube during rapid temperature changes (i.e.start-ups, operating issues, etc.) [5]. Repeated thermal cycling had resulted in the formation of thermal-based corrosion fatigue cracks.

A major difficulty with regard to fatigue research involves the large number of variables which influence the phenomenon. These may be divided into three general variables categories: mechanical, environmental and material [11]. Ramsamooj D. and Shugar T. presented an interaction between stress corrosion and additional parameters needed to predict corrosion fatigue might be applied mechanical stress, its frequency, and the threshold stress intensity factor phenomena, leading to an analytical expression for the corrosion fatigue in an aggressive environment for different metals [10]. In this work, it only consider the mechanical stress as a parameter but in boiler heat tube case there is thermal stress that might be taken as factor that affect the corrosion fatigue adversely.

In corrosion fatigue, the magnitude of cyclic stress and the number of times it is applied are not the only critical loading parameters. Time-dependent environmental effects also are of prime importance [14]. Seifer H.et al. have studied the corrosion fatigue crack growth behavior of different wrought low-carbon and stabilized austenitic stainless steels was characterized under simulated boiling water and primary pressurized water reactor conditions by cyclic fatigue tests with pre-cracked fracture mechanics specimens in the temperature range from 70°C to 320°C [14]. But their study have only focused on crack growth and limited range of temperature that may not be applied for boiler of steam power plant which can function up to 700°C.

Khaleel H. et al. have also studied the effect of temperature on corrosion rate of carbon steel was evaluated by weight loss analysis [16]. They have solely focused on the effect of temperature on the rate of corrosion in acidic solution.

In water-tube boilers, the water that circulates through the boiler tubes is externally heated by hot gases coming from the furnace resulting in generation of superheated steam. Since these machines operate at high temperature and at high-pressure environments, boiler tubes often suffer from a variety of failure mechanisms such as thermal fatigue and corrosion fatigue [17]. It has been determined that CFC is governed by interactions between loading, metallurgical, and environmental factors. Unlike environmentally assisted cracking (such as stress corrosion cracking), corrosion fatigue will generally occur in any alloy exposed to both a corrosive environment and cyclic stress [18].

Jinu G. et al. have experimentally investigated by laboratory simulation for producing the thermal fatigue phenomenon is developed to determine the number of cycles necessary before failure occurs in superheater tubes, where the tubes subjected to thermal cycles 800°C to room temperature [19]. They have studied thermal fatigue on ASTM A213 grade T-92 base and welded tubes by heating and cooling.

### **2.3 Review on Crack Propagation**

Many models have been proposed related to fatigue crack propagation. From those models, Paris law is a well-known model. This model is proposed by Paris and Erdogan in (1963) and is limited to describe only crack propagation in elastic strain range or for high cycle fatigue using stress intensity factor. So, Paris power-law do not apply for plastic strain range if not strain energy release rate or cyclic J-integral is used.

Foreman have suggested a new model which capable of describing region III of fatigue rate curve includes stress ratio effect. The limitation of this model it's sensitive to stress ratio R. And also Collis Priest (1972) proposed a crack growth law capable of describing all the regions includes stress ratio effect [34].

The other model is a model proposed by McEvily that relate the crack advance per cycle in the striation mode to the crack tip opening displacement and threshold effect [33]. It is useful only for lower portion of fatigue curve.

Frost and Pook hypothesized that the crack growth occurs under cyclic loading not as a consequence of any progressive structural damage but because of unloading reshapes the crack tip at each cycle [35]. However, experimental crack growth rates are underestimated at high growth rates and overestimated at low growth rates.

Wang et.al proposed a damage accumulation theory which considers plastic component of the J integral as damage factor resulting in a simple formula for fatigue crack growth rate, by taking assumptions: total plastic energy density absorbed by the material is a constant prior to reaching its ultimate state and the elastic strain energy density stored by the material does not cause damage and is released upon unloading [36]. This model conclude that crack growth is not only a function of stress intensity factor but also it is a function of an average of local yield strength, fracture toughness and amplitude of effective stress intensity factor in region II and

III. Additionally, Miller and Gallagher proposed the model which include crack initiation and stage I growth.

The above-discussed models have a common fracture  $\Delta K$ , assume LEMF is always valid. For a condition large scale yield, fatigue crack growth, the stress intensity factor no longer valid. Dowling and Bengley suggested to use  $\Delta J$  integral fracture parameter [36]. The equation is very similar to Paris equation however this equation used under a fatigue crack growth under large scale yielding conditions.

In this research, the prime targets are focusing on modeling the fatigue life of boiler tube that starts from volumetric growth rate of pit, then transited to small crack and propagate until failure. Low cyclic fatigue approach is used for crack propagation model since the system is subjected to high thermal stress and in this section of the model assumed there is pre-cracked surface.

Generally, for different conditions have been studied related to corrosion fatigue especially for aggressive environment, but it is difficult to say all conditions have covered. The models related to crack initiation and crack propagation have been discussed and model that appropriately describe the system is selected. Here temperature cause change in material property and alter the corrosion rate. In this research, all parameters which influence or affect the fatigue life will be considered and mainly focusing on those parameters that affect the rate of corrosion, crack nucleation or crack initiation and crack growth.

## **2.4 Research Gap**

Many researches were conducted related to corrosion and thermal stress that causes fatigue. However, the combined effects of corrosion, thermal stress as well as the high temperature that alter the rate of corrosion were not studied for 8.72Cr-0.9Mo steel as this material is suitable tube for power generation and steam generator industries. Corrosion and thermal stress are the parameters which adversely affect the life of boiler in power plants. Corrosion and those stresses are cause of corrosion fatigue, stresses yield stress intensity on tube surface which has pitting (flaw) by corrosion. This stress intensity causes stress corrosion cracking and later changed to corrosion fatigue. Thus, this research work modeled fatigue life of boiler heater

tube which operates under high thermal stress and corrosive media which generate corrosion pit. Mainly focusing on:

- Rate of corrosion or volumetric pit growth rate
- Crack initiation and pit to crack transition
- Crack propagation and fatigue life prediction of boiler heat tube

# Chapter

# 3

## Research Methodology

### 3.1 Introduction

A research methods are the strategies, processes or techniques utilized in the collection of data or for analysis in order to discover new information or create better understanding. The methodology explains what and how to do, allowing readers to evaluate the reliability and validity of the research. In this chapter, the methods and approaches of modeling the physical system will be discussed. The following figure summarizes the methods used during conducting this study in flow diagram form.

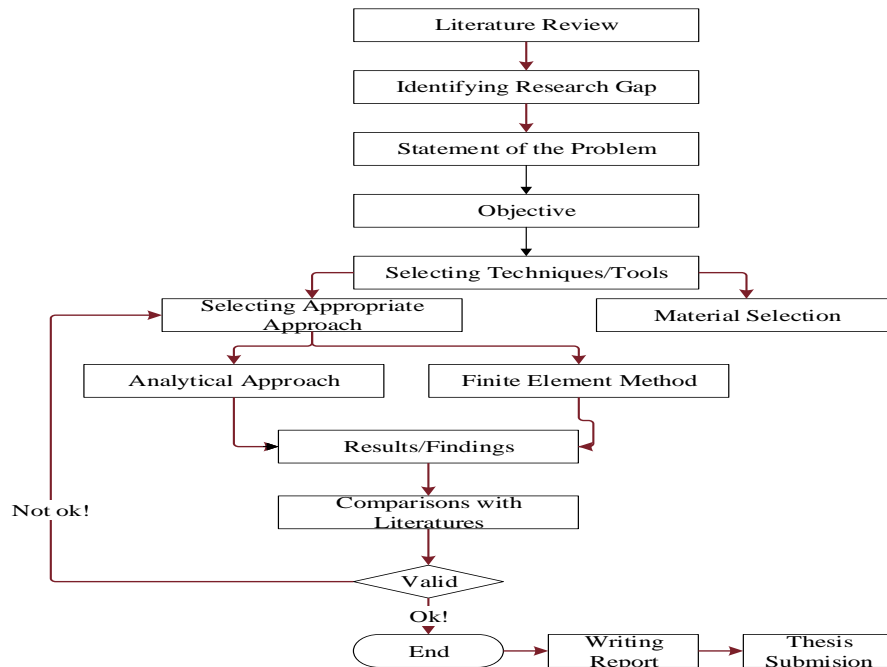


Figure 3. 1 Flow diagram of research methods

### **3.2 Selection of Appropriate Approach**

There are various methods that can be used to conduct research and these can be either quantitative, qualitative or combination of both (mixed method). This study is quantitative in nature which mathematically model fatigue failure of boiler heat tube and analysis performed using results.

Conducting the experiment for fatigue is so expensive, economically not feasible and time-consuming. Using mathematical model and software package is very appropriate in such type of research area.

### **3.2 Tools or Techniques**

Modeling is the description of systems using mathematics. Mathematical models are usually composed of relationships and variables and modeling will be conducted using software packages. Modeling effect of temperature on the rate of corrosion is a dynamic modeling where the rate of reaction change with time. Total fatigue life is the summation of the number of cycles crack initiation  $N_i$  and the number of cycles crack propagation  $N_p$  to failure.

There are different crack propagation modeling can be used in fracture mechanics. For linear elastic functionally graded materials (FGMs), fracture parameters can be described stress intensity factor (SIF) and T-stress (non-singular stress). These two fracture parameters modeling are important for determining the crack initiation angle under mixed-mode loading condition in brittle FGMs (e.g. ceramic). J-integral is another model used to describe crack propagation in large plastic strain deformation under cyclic loading, which is non-linear crack propagation, and also can used for a materials subjected high thermal stress that result low cycle fatigue. So, J-integral method used for crack propagation which is appropriate and preferable approach.

Software analysis have done using ABAQUS software package. 3D modeling of parts, simulation thermal stresses, and simulation of crack propagation have used ABAQUS software.

### **3.3 Data Processing, Analysis and Interpretation Techniques**

Data processing is the collection and manipulation of items of data to produce meaningful information. Software can be used to process, analysis and interpret input data to detectable or



meaningful information to the reader. This study have formulated the mathematical model for fatigue life; under this modeling, the rate of corrosion, crack nucleation (initiation), crack propagation and predicting the life of boiler heat tube, the analyzing and interpret the results.

Software simulation have also conducted using ABAQUS software package. This study have compared the results of mathematical model and software simulation.

### 3.4 Materials

The material that used for this research is high chromium steel of modified 9Cr-1Mo steel heater tube which have a size of outside diameter of 32mm and inside diameter 28mm and the size of the heat tube is randomly selected (Appendix B). 8.72Cr-0.9Mo steel is ferrite grade steel, with manufacturing standard ASTM has good thermal properties and corrosion resistance, which is mostly used in power generation and having tensile strength 669Mpa, yield strength 533Mpa and hardness of 89 Rockwell mechanical properties.

The materials are characterized by different conductivity, temperature, and steam oxidation. The properties have a significant impact on their performance in steam conditions.

Table 3. 1 Chemical Composition of 8.72Cr-0.9Mo steel (T91) Steel [42]

| <b>C</b> | <b>Si</b> | <b>Ni</b> | <b>Mn</b> | <b>P</b> | <b>Cr</b> | <b>S</b> | <b>Mo</b> | <b>V</b> | <b>N</b> | <b>Nb</b> | <b>Fe</b> |
|----------|-----------|-----------|-----------|----------|-----------|----------|-----------|----------|----------|-----------|-----------|
| 0.096    | 0.32      | 0.1       | 0.46      | 0.012    | 8.72      | 0.006    | 0.90      | 0.22     | 0.051    | 0.08      | Bal.      |

Table 3. 2 Mechanical Properties of 8.72Cr-0.9Mo steel T91 Steel [43]

| <b>Tensile strength</b> | <b>Yield strength</b> | <b>Elongation</b> | <b>Rockwell Hardness</b> |
|-------------------------|-----------------------|-------------------|--------------------------|
| 669Mpa                  | 533Mpa                | 27%               | 89                       |

## Chapter

# 4

## Analytical modeling and finite element simulation

### 4.1 Introduction

There are different methods used to solve problems and/or to describe the phenomena of the systems. In engineering field, experimental investigation, collecting data and surveying, analytical approach and finite element method (FEM) are common methods that are used. In this study analytical method and finite element method are used.

Large number of structural components in engineering area are subjected to a wide variety of loads of mechanical and thermal origin. The phenomenon of fatigue may be induced by a cyclic thermal loading. Thermal stresses play an important role in various fields of industries and power generation plants. In power generation plants, corrosion pitting is the main problem. The combination of thermal load and corrosion pitting reduce the fatigue life of the components. This chapter deal with pit growth rate under temperature influence, pit to crack transition and crack propagation. Analytical approach and finite element method are used.

Mathematical modeling is a representation in mathematical terms of the behavior of real devices and objects. Since the modeling of devices and phenomena is essential to both engineering and science, engineers and scientists have very practical reasons for doing mathematical modeling [48]. Mathematical modeling is a principled activity that has both principles behind it and methods that can be successfully applied.

Simulation software helps to predict the behavior of a system. To run a simulation, a mathematical model of system, which can be expressed as a block diagram, schematic, statechart, or even code can be used. The simulation software calculates the behavior of the model as conditions evolve over time or as events occur. Simulation software also includes

visualization tools, such as data displays and 3D animation, to help monitor the simulation as it runs.

## **4.2 Analytical approach**

Analytical models are mathematical models that have a closed-form solution. The solution to the equations used to describe changes in a system can be expressed as a mathematical analytical function [47]. More than anything else, an analytical approach is the use of an appropriate process to break a problem down into the smaller pieces necessary to solve it. Each piece becomes a smaller and easier problem to solve. There are a number of analytical methods to determine fatigue life the material:

- (i) The stress-life method,
- (ii) The strain-life method,
- (iii) The crack growth method and
- (iv) Probabilistic methods, which can be based on either life or crack growth methods.

Stress-life based method is used in high cycle fatigue (HCF) and strain-life based method is used for low cycle fatigue (LCF) when strains are no longer elastic, such occurs due to the presence of stress concentrations, the total strain can be used instead of stress as an amplitude parameter. And there are a models that developed to describe crack growth phenomenon.

### **4.2.1 Basic Assumptions**

Operational boiler tubes may be considered as thin-walled cylindrical tube which subjected to thermal stress and corrosion media. To avoid complexity in engineering, different assumption should be taken. The following assumption is taken throughout the document:

- i. The material is homogeneous and isotropic
- ii. Material properties is temperature-dependent
- iii. Corrosion cause pitting which later changed to crack
- iv. Radial stress is assumed to be zero since the wall thickness is small when compared to diameter of tube
- v. Circumferential (hoop) stress and longitudinal (axial) stress is used throughout analysis
- vi. Plastic deformation at crack tip

- vii. Plane-strain analysis
- viii. There is no creep-fatigue since creep is activated at half the melting point of the metals

#### 4.2.2 Temperature-Dependent Material properties

Mechanical characteristics of most materials are greatly influenced by the operating temperature. Thermo-mechanical properties of materials are studied for the prediction of material behavior in wide range of parameters characterizing their internal state (for example, temperature and deformation) and structure (for example porosity or permeability). Changes of state parameters and structural characteristics of a material are caused by exchange and mechanical interaction of a material with environment. Thermo-mechanical properties of materials which study is required for many practical applications are heat capacity, thermal conductivity, rheological properties, thermal expansion, and strength.

Young’s modulus is temperature-dependent parameter or material properties which changes with temperature. Equation (4.1) describes this change as a function of temperature.

$$\frac{E(T)}{E(20)} = 1.0 + \frac{T}{2000 \ln\left(\frac{T}{1100}\right)} \quad \text{for } 20^{\circ}\text{C} \leq T \leq 600^{\circ}\text{C} \quad (4.1)$$

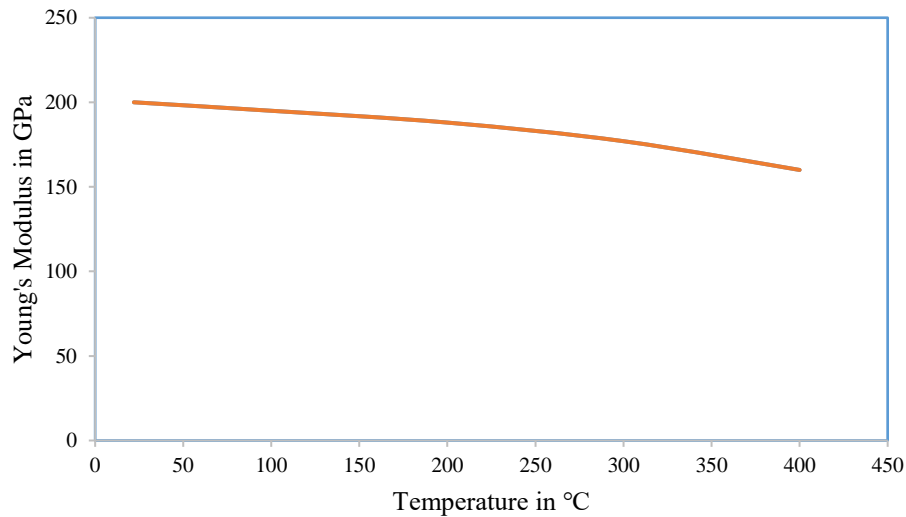


Figure 4. 1 Young’s modulus response to change in temperature

Young's modulus, poisson's ratio, and thermal expansion coefficient are temperature-dependent parameters. Young's modulus decreases with temperature as shown in figure (4.1). However, poisson's ratio is do not change with significant value in this range of temperature.

$$\nu=3.78 \times 10^{-5} T+0.283 \quad \text{for } 0 \leq T \leq 450^{\circ} \text{C} \quad (4.2)$$

Before proceeding to modeling the fatigue initiation and crack propagation of this type of fatigue, it is important to know what are the value of cyclic stress and strain since those parameters are the input for the model.

### 4.2.3 Thermal Stress (Circumferential and Longitudinal Stress)

As a solid material experiences an increase in temperature, the volume of the structure is ultimately impacted by increasing, a phenomenon known as thermal expansion. Within solids, molecules are typically located close proximity to another, contributing for the whole structure. As a temperature rises, molecules begin to vibrate at a more rapid speed and push away from one another. This increased separation between the individual atoms causes the solid to expand. With this volumetric enlargement, the elements of a solid undergo greater levels of stress.

The stress-induced by thermal when the boiler tube is subjected thermal load. During application of thermal load, the tube get expand on side the heat applied surface. If the heat applied on outer surface of the tube, the tube get expand at outer surface and get compressed inner surface. Taking small portion of the tube and considering as flat surface, thermal stress can be written as equation (4.3). It is interested here focusing only on in the maximum value of stress and by making the radial stress zero  $\sigma_r = 0$ . Thermal stress in tube during heating and cooling both axial and circumferential stress will be equal and calculated as follow:

$$\sigma_a = \sigma_{\theta} = \pm \frac{\alpha E (T_o - T_i)}{2(1-\nu)} \quad (4.3)$$

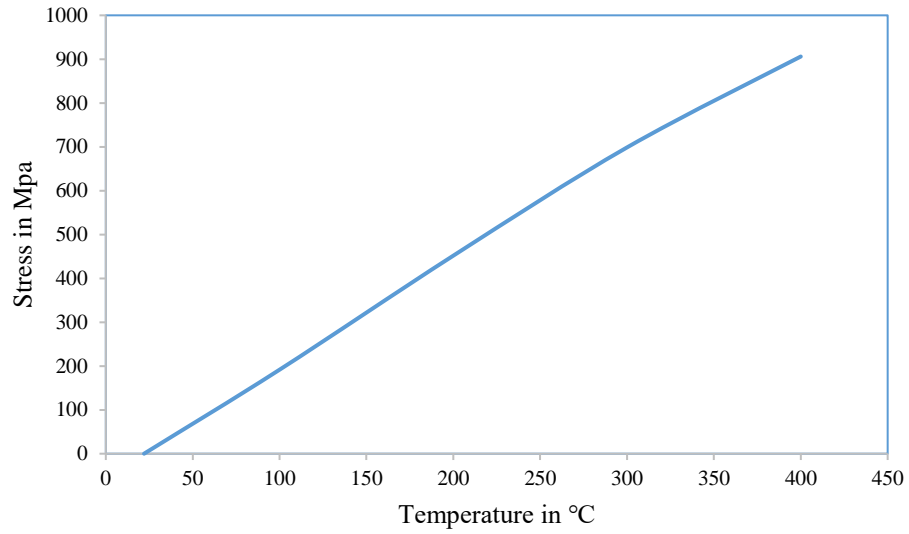


Figure 4. 2 Response of stress to temperature change

Where  $\sigma_a$  is axial/longitudinal stress,  $\sigma_\theta$  is circumferential stress,  $E$  is young's modulus of material,  $\nu$  is poison's ratio and  $\alpha$  thermal expansion coefficient.

#### 4.2.4 Temperature distribution through thickness

Since there is a temperature gradient across the thickness of the tube, when inner surface of the tube heated it expand but the outer part of tube resist this expansion. So, the outer surface

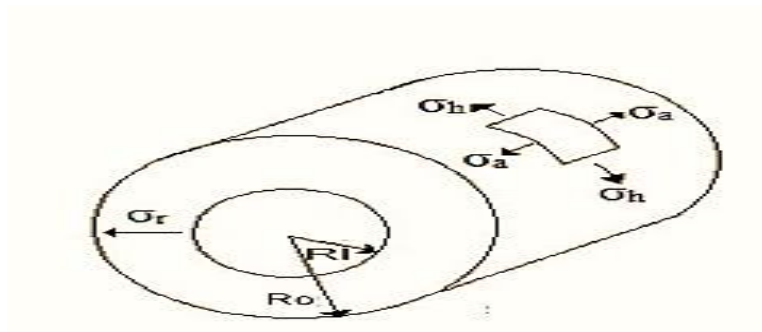


Figure 4. 3 Stress induced on outer surface of heat tube

subjected to tensile load or stress. The temperature distribution through the thickness of the cylinder is given equation (4.4)

$$T = T_i + \frac{(T_o + T_i)}{\ln(R_o/R_i)} \ln(R/R_i) \quad (4.3)$$

Where  $R_o$  is the outer radius,  $R_i$  is the inner radius,  $T_o$  is the outside temperature and  $T_i$  is the inside temperature. In equation (4.4), temperature change insignificant when the thickness of the wall is very small.

#### 4.2.5 Thermal Strain

Temperature change can also cause strain. In anisotropic material, the thermally induced extension strains are equal in all directions, and there are no shear strains. When cylinder wall is very small relative to its diameter, then it is possible to take an assumption and treat the cylinder as a plate. Circumferential strain and axial strain can be calculated using equation (4.5) and equation (4.6) as shown below.

$$\varepsilon_\theta = \frac{1}{E} [\sigma_\theta - \nu(\sigma_r + \sigma_a)] + \alpha\Delta T \quad (4.4)$$

$$\varepsilon_a = \frac{1}{E} [\sigma_a - \nu(\sigma_r + \sigma_\theta)] + \alpha\Delta T \quad (4.5)$$

Where  $\varepsilon_\theta$  is circumferential strain,  $\varepsilon_a$  is axial/longitudinal strain and  $\sigma_r$  is radial stress. Radial stress is assumed to be zero since tube has small wall thickness. So, radial strain become zero.

The above equation becomes

$$\varepsilon_\theta = \frac{1}{E} [\sigma_\theta - \nu\sigma_a] + \alpha\Delta T \quad (4.6)$$

$$\varepsilon_a = \frac{1}{E} [\sigma_a - \nu\sigma_\theta] + \alpha\Delta T \quad (4.7)$$

Since crack occur on surface of the tube and with very small size, no need to take the strain of the whole tube. For very small area of tube the tube surface approximately flat surface so it is possible to assume the surface as a flat surface. Equation (4.7) and equation (4.8) reduced to the following equation (4.9).

$$\varepsilon_\theta = \varepsilon_a = \alpha\Delta T \quad (4.8)$$

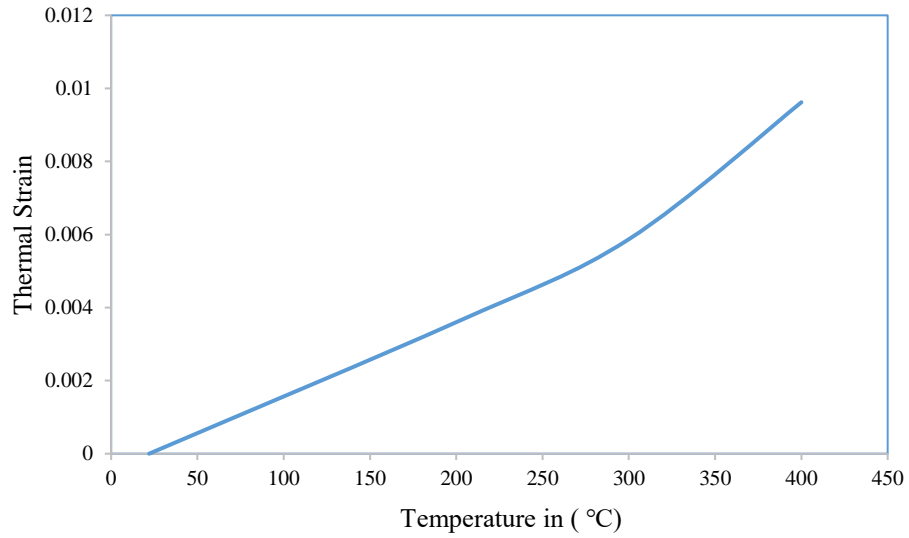


Figure 4. 4 Response of thermal strain to change in temperature

#### 4.2.6 Load Cycles

Load cycles can be applied in a variety of wave shapes, from the sinusoidal shape triangular, squared or even an irregular shape. Stress can go from maximum to minimum or vice-versa and it can be negative or positive. For instance, if the applied load is tensile it is considered as  $\sigma_{\max}$  positive and if applied load is compressive  $\sigma_{\min}$  considered as minimum. When both  $\sigma_{\max}$  and  $\sigma_{\min}$  are in positive the cycle will be positive.

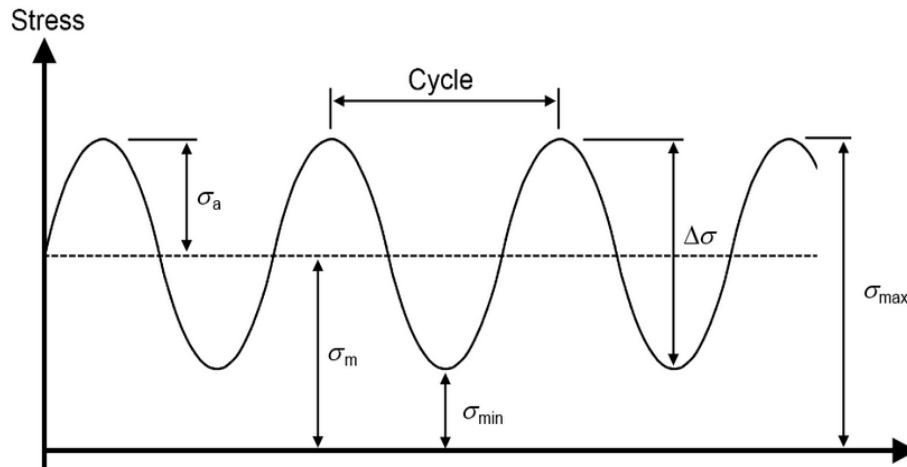


Figure 4.5 Sinusoidal load cycles



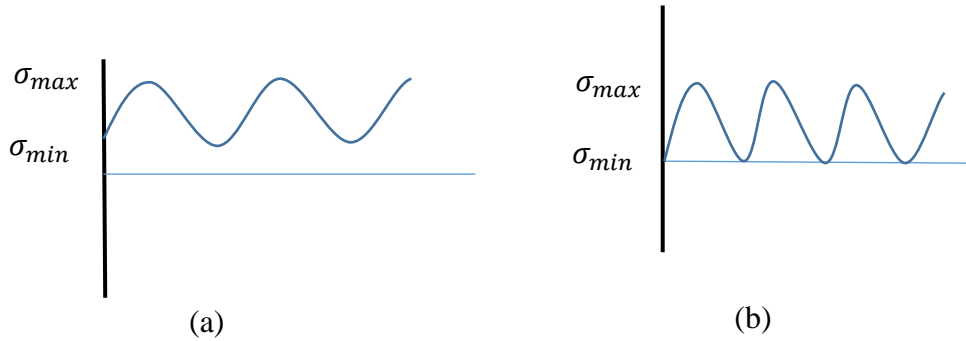


Figure 4. 6 Cyclic load. (a) load with both  $\sigma_{max}$  and  $\sigma_{min}$  positive (b) load with  $\sigma_{max}$  and  $\sigma_{min}$  zero

The applied stress is elastic, fatigue phenomenon is considered to be high cycle fatigue (HCF) where  $N > 10^5$  cycles and when the stress on the component is high enough to cause plastic deformation, the phenomenon is known as low cycle fatigue (LCF). This model assumes power plant operates for 8 hours per day. So there is cyclic heating and cooling of the heater tube that leads to fatigue of the component. The stress range will be from zero to maximum, since it cool to room temperature and reheat up again.

The effect of corrosion will be determined for fatigue endurance of materials, as corrosion could cause a faster crack initiation, a higher crack propagation rate or both. Since corrosion attacks the surface of the part, corrosion fatigue cracks will always originate at the surface, unless the material presents defects underneath the surface, which would act as stress concentration sites and initiates sub-surface cracks. Corrosion fatigue cracks usually trans-crystalline and although inter-crystalline cracks can nucleate if the media attacks the grain boundaries preferentially.

#### 4.2.7 Low Cyclic fatigue

S-N curve can be divided into three regions. In region I, from 1/4 cycle to about  $10^4$ - $10^5$  cycles, the material is stressed in the vicinity or beyond the yield stress. The material deforms plastically and the plastic strain dominates the fatigue life. Region I is often referred to low cycle fatigue and concern of this research because there is initially a crack by corrosion (pitting). In region II, the material behaves elastically, at least at the macroscopic level. The stress amplitude is lower than the yield stress of the material. Region II goes up to  $10^6$  or  $10^7$

cycles. Region III is loosely defined as the region for which failure does not occur either for a specified number of cycles or at all.

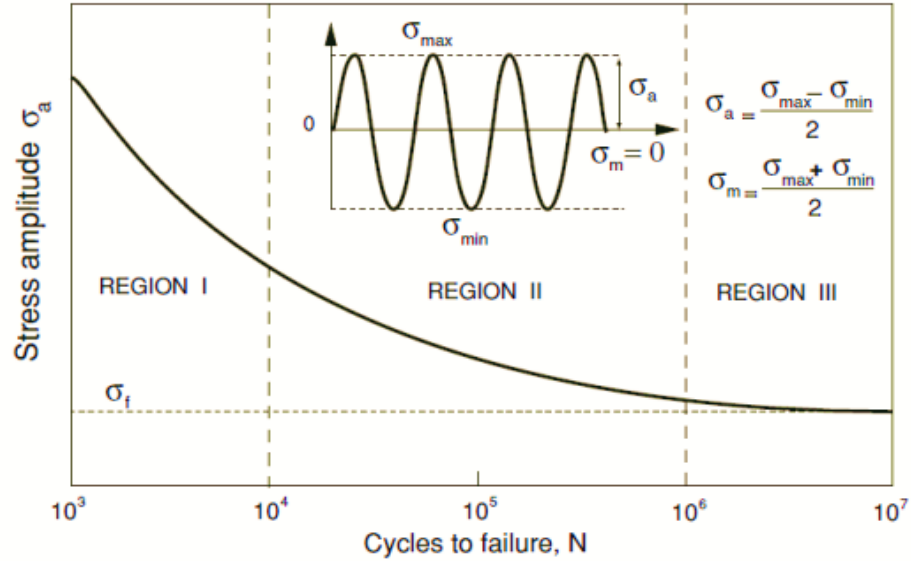


Figure 4. 7 A schematic of typical S-N curve showing the stress amplitude versus cycles to failure [after:21]

Paris and Erdogan have been proposed the expression which govern fatigue crack propagation rate. However, this expression is limited elastic strain range fatigue (region III) which do not describe plastic strain range or region I.

$$\frac{da}{dN} = C(\Delta K)^m \quad (4.9)$$

In the range of low cycle fatigue (LCF), it do not obey the Paris law using stress intensity factor, i.e. the rate failure is high not governed by this law [18]. Foreman have developed the equation that can account for this case.

$$\frac{d_a}{d_N} = \frac{C(\Delta K)^m}{(1-R)K_c - \Delta K} \quad (4.10)$$

$$\Delta K = Y\Delta\sigma\sqrt{\pi a} \quad (4.11)$$

Where: a is the flaw or crack size; n is the number of cycles; C and m are constant parameters and are related to material variables, environment, temperature, and fatigue stress conditions.

Typically,  $m$  is in the range of 2 to 4 for metals. Fatigue cracks in service usually grow in a direction which is macroscopically perpendicular to the main stress.

The above expression do not work for this case because minimum stress here considered to be zero and stress ratio becomes zero and critical stress intensity and threshold stress intensity are equal, which yields the total cancelation of the equation. As a result, it is preferable to use J-integral expression which based on crack opening displacement under excessive plasticity. J-integral approach used to predict elastic-plastic fracture and non-linear behavior is prominent in nuclear power industry (pressure vessels and piping). And also used in elevated temperature application like boiler of power plants.

The plastic strains are responsible for the LCF damage as established independently by Coffin and Manson [21]. They proposed an empirical relationship between the number of load reversals to fatigue failures and the plastic-strain amplitude. This so-called Coffin-Mansion relationship has remained the most widely used total-fatigue-life approach to LCF.

#### 4.2.8 Modes of Failure

Three linearly independent cracking modes are used in fracture mechanics. These load types are categorized as Mode I, II, or III as shown in the figure 4. Mode I, shown to the left, is an opening (tensile) mode where the crack surfaces move directly apart. Mode II is a sliding (in-plane shear) mode where the crack surfaces slide over one another in a direction perpendicular to the leading edge of the crack. Mode III is a tearing (anti-plane shear) mode where the crack surfaces move relative to one another and parallel to the leading edge of the crack. Mode I is the most common load type encountered in engineering design. Mode I is the concern of this study which is under thermal tensile stress.

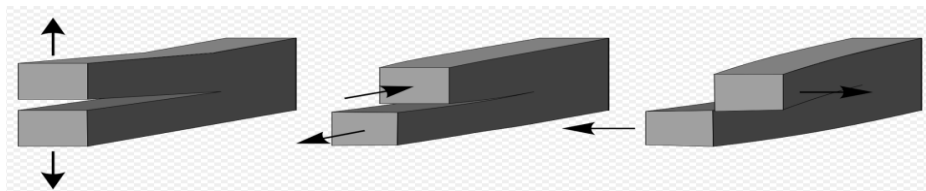


Figure 4. 8 Opening or mode I (left), sliding or mode II (middle) and tearing or mode III (right)

## 4.3 Crack Initiation

In material science, fatigue weakening of material. It is a cumulative effect that causes a material to fail after repeated applications of stress, none of which exceeds the ultimate tensile strength. There different types of reasons to initiate crack. A factors like porous during manufacturing, corrosion pitting, flaw happen under operation and other factors. Cracks start at the surface of the material where the highest stress is normally found. SCC frequently initiates at preexisting or corrosion-induced surface features or pits formed during exposure to service environment. Repeated stressing accelerates the corrosive action and corrosive action accelerate the mechanical/thermal fatigue mechanisms. Corrosion in fatigue is an electrochemical process dependent on the environment/material stress interaction. Figure (12) shows formation elliptical pit on the surface of tube and progressive growth of pit. In boiler tube the rust  $\text{Fe}_2\text{O}_3 \cdot x\text{H}_2\text{O}$  (iron oxide) which is transported to another surface of the tube is eroded by pressured water inside the system.

### 4.3.1 Corrosion Rate

Metals undergo a chemical change when exposed or contact with environment like air or water. This chemical change decreases the integrity of the metal. Due to that, the metal cannot hold the same load as before. The most common kinds of corrosion results from electrochemical reactions. General corrosion occurs when most or all of the atoms on the same metal surface are oxidized, damaging the entire surface. Most metals are easily oxidized, they tend to lose electrons to oxygen (and other substances) in the air or in water. As oxygen is reduced (gains electrons), it forms an oxide with the metal.

The rate of corrosion is the speed at which any given metal deteriorates in a specific environment. The speed is depends on environmental condition and types of metal. Corrosion behavior of a material is quantitatively expressed in terms of corrosion rates. The parameters, which affect the corrosion rate of a material, can be broadly classified as:

- (i) Solution chemistry (Environmental): concentration, pH, temperature, velocity, conductivity, presence of foreign ions, aging of the medium, exposure period, type of exposure (alternate, partial, total submersion, etc.), bacteria, microbes, etc.
- (ii) Metallurgical: microstructure, grain orientation, texture, alloy composition and purity, presence of defects, etc.

- (iii) Mechanical presence of stress (applied, residual and thermal), rate of application, type of stress (tensile, compression or cyclic), strain rate, notches, application of stress before or after exposure to medium, etc.

Many parameters affect the rate of corrosion but in boiler temperature and moisture at the inside, the tube are a critical parameters which affect the rate of corrosion.

Since condensed water feed into the boiler, this condensed water moist the surface of tube and facilitate environment for corrosion. The assumption taken in this paper is, high corrosion rate will happen at tube bends, where it very facilitate corrosion to occur.

It is known that electrochemical process of corrosion of steel consists of two mutual conditions coupled anodic and cathodic reactions. Figure (4.9) shows the two mutual reaction under moisture environment or containing water which facilitates the occurrence of corrosion.

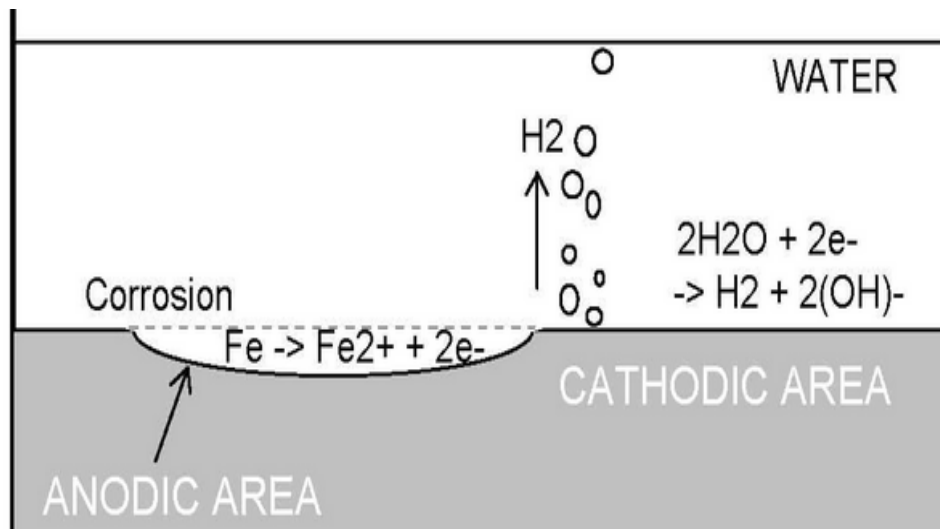
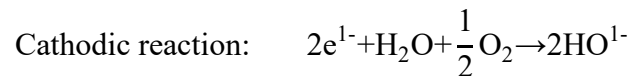


Figure 4. 9 Anodic and cathodic reaction the metal under corrosion [41]



Corrosion in steel consists of solid iron, liquid water, and gaseous reactants. Two reactants of steel corrosion, water and oxygen are sensitive to temperature changes. According to Zivica

V. as a temperature increased the solubility of oxygen in water significantly decreased and water vapor tension significantly increased [25].

### 4.3.2 Effect of Temperature on Corrosion

Pressure variable include, pressure volatile product and pressure of reactant in gas-solid reaction has a significant effects on rate of reaction. However, compared to temperature the pressure variable do not change the rate of reaction, even if it is gas-solid reaction.

An increase in temperature will generally increase the rate of corrosion. A rule of thumb is that temperature increases of  $10^{\circ}C$  will double the corrosion rate. Thus, corrosion rate can be described using Arrhenius equation follow

$$CR=A\exp^{-E_a/RT} \quad (4.12)$$

Taking natural logarithm both side's equation and it gives equation (4.14)

$$\ln CR=\ln A-E_a/RT \quad (4.13)$$

Using this equation if corrosion rate at room temperature is known it can be predict the rate at any temperature of the boiler. Where CR is corrosion rate of carbon steel ( $\mu\text{m}^2/\text{s}$ ) or rate constant derived from metal loss data.  $E_a$  is Activation energy (J/mole), R is gas constant (8.314J/mole.k) and T is temperature (k). From this equation, it is clearly seen corrosion rate (CR) depends on temperature. Activation energy is identified as the energy barrier which must be surmounted (overcome) during the bond redistribution steps required to change reactants into products. A is frequency of occurrence of high energy configuration.

The graph below shows change of corrosion rate with change in temperature for the temperature interval of  $50^{\circ}C - 600^{\circ}C$ . It clearly seen increasing temperature increase the rate of corrosion. For some interval of the temperature smoothly increase, and then as temperature increase above  $350^{\circ}C$ , the rate increased sharply. After  $500^{\circ}C$  it increases smoothly.

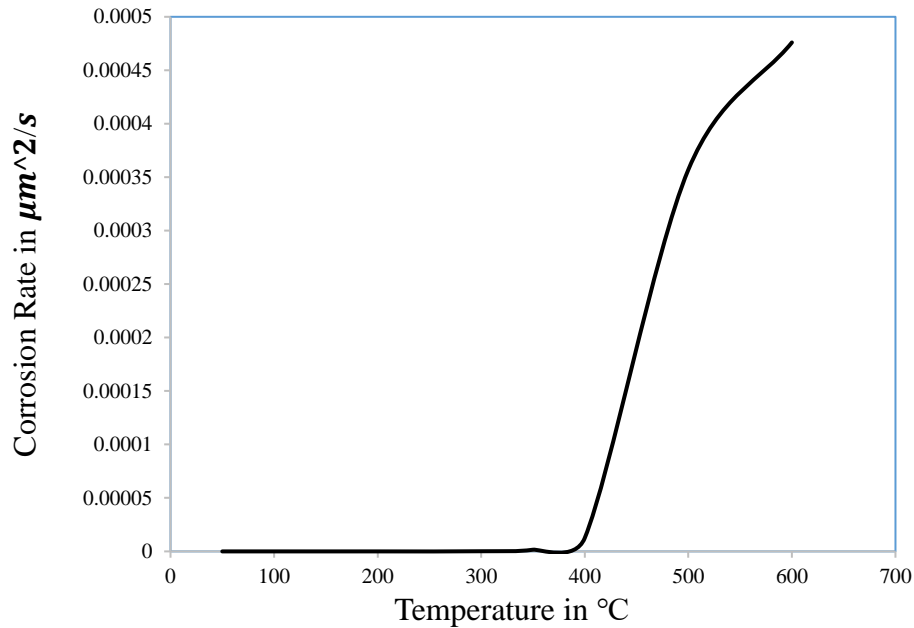


Figure 4. 10 Change of corrosion rate with temperature

### 4.3.3 Pitting

Corrosion pitting is characterized by the formation of small cavities (pits) in the metal. Pitting is often difficult to detect and monitor. The main cause of pitting phenomena is the formation of a stable corrosion, on the surface of a passive metal, as a result of breakdown or perforation of protective oxide layer. In this cell, the passive area plays the role of a cathode when the metal bottom in pit actively dissolves as an anode.

Pitting is a type of extremely localized attack. Pitting is a destructive form of corrosion that affects the waterside of boiler tubes. Surface imperfections and deposits can serve as initiation sites of pitting, and a consequent breakdown of protective scale. The corrosive penetration depends on factors such as temperature, oxygen concentration and lack of fresh fluid to the pitted area.

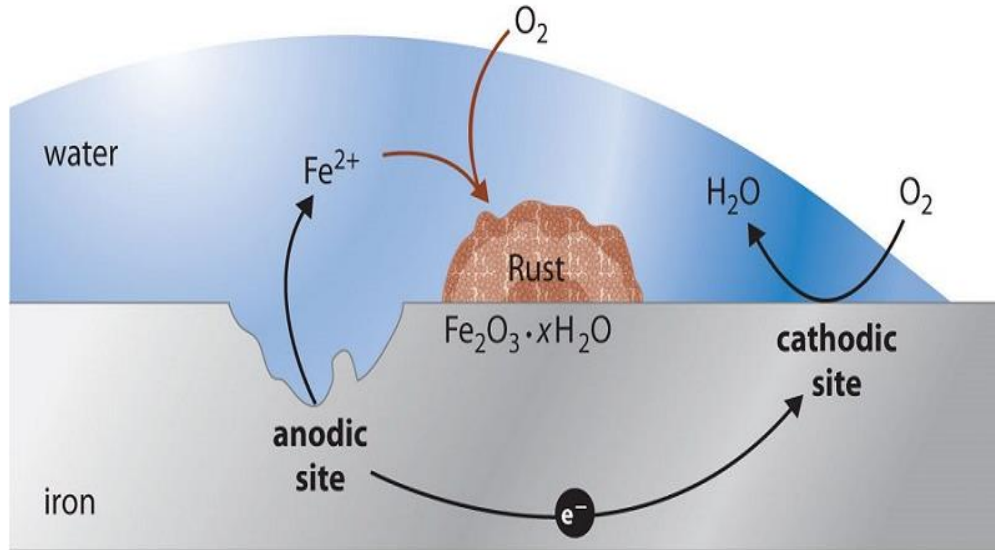


Figure 4. 11 Pit formation [41]

#### 4.3.4 Pit to Crack Transition

Corrosion induce the pit on the surface of tube and which is later changed to small crack by the action of cyclic stresses. Here the model assume as there is existing pits used as an input for crack initiation, which is described by pit to crack transition. Number of stress cycles  $N$  required for failure of heat tube is the summation of number of cycle required pit to crack transition  $N_{in}$  and number of cycles required for crack propagation  $N_p$ .

$$N=N_{in}+N_p \quad (4.15)$$

In normal non-corrosive environment, most of fatigue lifetime is exhausted in crack initiation. But in the presence of corrosion, it reduce greatly the life that take to crack initiate, since the flaw surface or pitting generated by corrosion accelerate the rate of crack initiation.

According to Akid, there are four stages of the fatigue lifetime of the materials:

Stage 1: Surface film breakdown

Stage 2: Pit growth

Stage 3: Pit to crack transition

Stage 4: Cracking (includes both short and long crack growth)



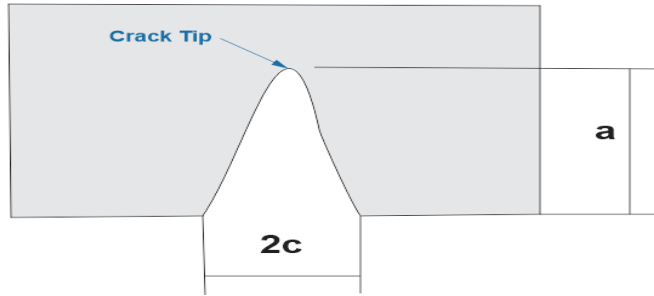


Figure 4. 12 Elliptical pit opening and its depth or length

Kondo has proposed that experimentally, opening radius of corrosion pit ( $c$ ) can be described using the equation below

Considering pit as semi-ellipsoidal, the volume of this pattern can be calculated using equation (4.16)

$$V = \frac{2}{3} \pi c^2 a \quad (4.16)$$

And taking aspect ratio pit opening radius to pit depth  $\alpha = c/a$ , then

$$V = \frac{2}{3} \pi \alpha^2 a^3 \quad (4.17)$$

According to Faraday's law pit grow at a constant volumetric growth rate can be written by equation (4.18). This expression indicates the rate is increased with increasing temperature.

$$\frac{dV}{dt} = C_p = \frac{M I_p^0}{n F \rho} \exp\left(-\frac{\Delta H}{RT}\right) \quad (4.18)$$

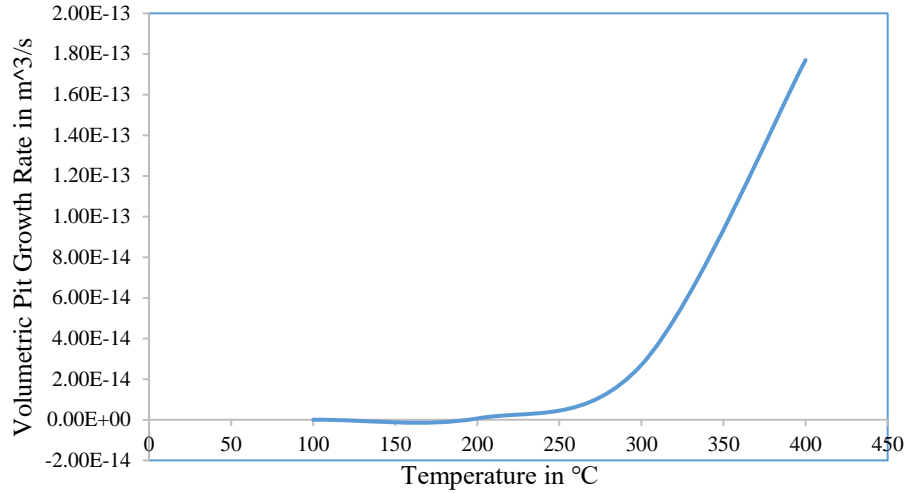


Figure 4. 13 Volumetric pit growth rate at different temperature

Substituting and differentiating the above expression gives, where M is molecular weight of the material, R is universal gas constant,  $\Delta H$  is activation energy and T is absolute temperature.

$$C_p = \frac{d\left(\frac{2}{3}\pi\alpha^2 a^3\right)}{dt} \quad (4.19)$$

$C_p$  Is volumetric pit growth rate, so that, the pit depth will be as follow

$$a = \left(\frac{3C_p}{2\pi\alpha^2}\right)^{1/3} t^{1/3} \quad (4.20)$$

Pit growth and initiation influenced by fatigue stress, model developed by Ishihara et.al [31] as

$$a = \left(\frac{3C_p}{2\pi\alpha^2}\right)^{1/3} t^{1/3} C^{\sigma_a} \quad (4.21)$$

For different values of aspect ratio,  $\alpha$  stress intensity factor should be different, assuming that  $\alpha \leq \frac{1}{2} C$  is constant related to material it ranges between 1.002 to 1.02 and the stress intensity factor can be written as:

$$\Delta K = 0.51 K_t \Delta \sigma \sqrt{\pi a / Q} \quad (4.22)$$

$$Q=1+1.146(\alpha)^{1.65} \quad (4.23)$$

Q is geometric correction factor (shape factor) and Cerit et al. proposed the relationship between aspect ratio and stress concentration factor by using finite element analysis [27] as:

$$K_t = \frac{\alpha + 3.33}{\alpha + 1} \quad (4.24)$$

The graph below shows stress intensity factor at pit tip at different cyclic loads. This result indicates stress at crack tip increases with pit size. The response is more pronounced at large cyclic load, implies the load causes large deformation at pit tip.

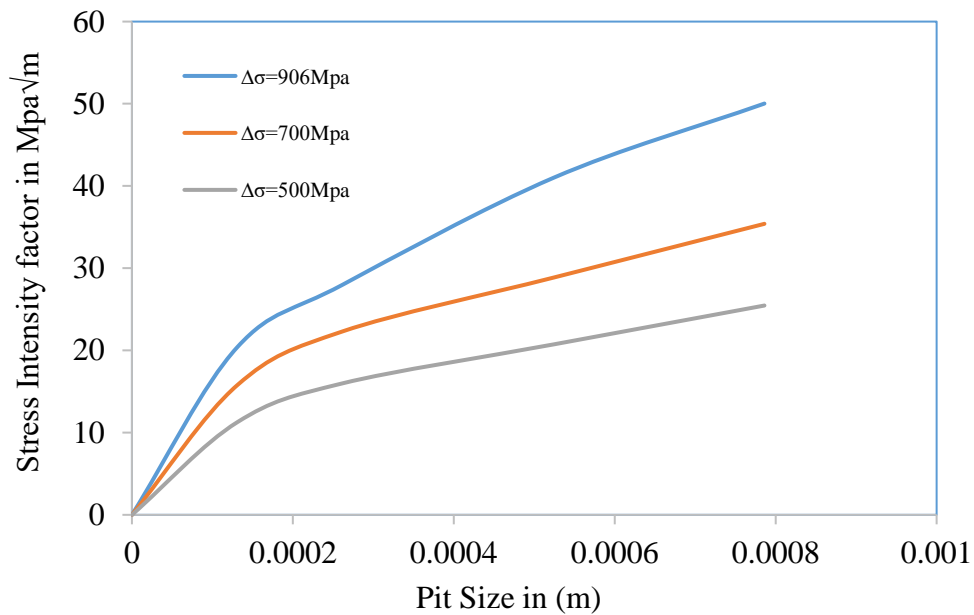


Figure 4. 14 Change of stress intensity factor and pit size at different cyclic stress

Here the assumption is maximum intensity factor is equal to fracture toughness of the material since the approach is stain based approach so that there is large plastic strain at the tip of the crack.

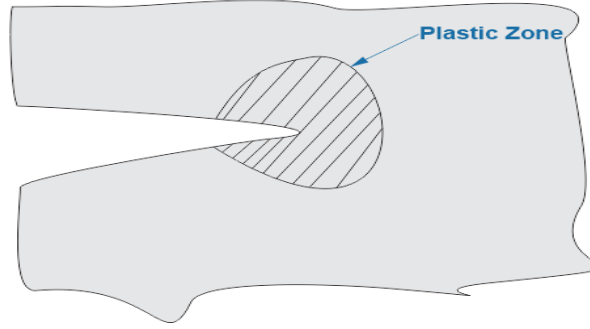


Figure 4. 15 Plastic zone for semi-ellipsoidal crack

$$\Delta K \sim K_C$$

Critical pit depth  $a_{cr}$  for crack initiation can be expressed as follow by substituting  $\Delta K = \Delta K_{cr}$

$$a_{cr} = \frac{Q}{\pi} \frac{(\Delta K_{cr})^2}{(0.51K_t \Delta \sigma)^2} = \frac{Q}{\pi} \left( \frac{\Delta K_{cr}}{0.51K_t \Delta \sigma} \right)^2 \quad (4.25)$$

Then by equating  $a = a_{cr}$  from the above equation, substituting the values for known parameters, then critical pit depth become  $a_{cr} = 0.524 \text{ mm}$  and the crack volume at transition instant is  $7.53 \times 10^{-11} \text{ m}^3$ .

$$\frac{Q}{\pi} \left( \frac{\Delta K_{cr}}{0.51K_t \Delta \sigma} \right)^2 = \left( \frac{3C_p}{2\pi\alpha^2} \right)^{1/3} t^{1/3} C \sigma_a \quad (4.26)$$

Solving for t gives a time takes to crack initiation written as the following expression

$$t = \left( \frac{Q}{\pi} \right)^3 \frac{2\pi\alpha^2}{3C_p C^3 \sigma_a} \left( \frac{\Delta K_{cr}}{0.51K_t \Delta \sigma} \right)^6 \quad (4.27)$$

So the number of cycles to initiate the crack will be

$$N_{in} = \frac{2\alpha^2 Q^3}{3C_p \pi^2 C^3 \sigma_a} f \left[ \frac{\Delta K_{cr}}{0.51K_t \Delta \sigma} \right]^6 \quad (4.28)$$

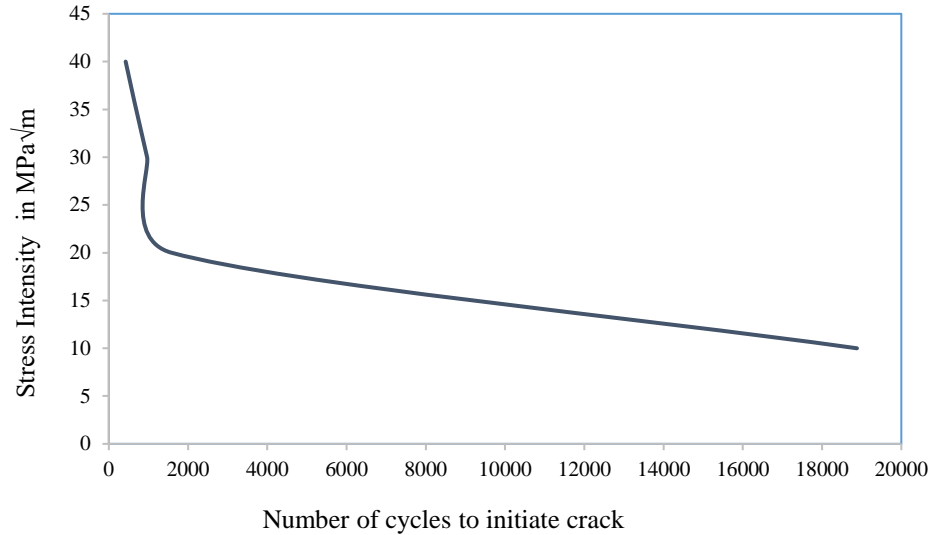


Figure 4. 16 Number of cycles to initiate crack

## 4.4 Crack Propagation

Crack propagation is a process of evolutionary geometry driven by relatively high values and gradients in crack front fields and concomitant material damage. It is believed that the corrosion fatigue crack propagation is caused by the combination of corrosion damage and relative slip of the metal at the crack tip under cyclic loading. Crack is propagated by the action of cyclic thermal load, which leads to large plastic deformation at the crack tip.

Crack growth is depends on several factors, such as bulk material properties, body geometry, crack geometry, loading distribution, loading rate, loading magnitude, environmental conditions, and microstructure. Those factors affects the rate of crack propagation, in this study material properties which change with temperature, magnitude of loading (thermal stress) and environmental condition are the prime focus.

### 4.4.1 Prediction of Strain based fatigue life using Manson and Coffin Equation

The structural components used at high temperature shows LCF failure as a predominant failure mode Low-cycle fatigue conditions are created when the repeated stresses are of thermal origin. Since thermal stresses arise from the thermal expansion of the material, it is easy to see that in this case, fatigue results from cyclic strain rather than from cyclic stress [21].

Total strain amplitude is the sum of the elastic and plastic components. Therefore strain amplitude is half the total strain range.

$$\frac{\Delta\varepsilon}{2} = \frac{\Delta\varepsilon_e}{2} + \frac{\Delta\varepsilon_p}{2} \quad (4.29)$$

Equation of the plastic-strain line proposed by Manson and Coffin and equation of elastic strain line proposed by Basquin given below

$$\frac{\Delta\varepsilon_p}{2} = \varepsilon_f (2N)^c \quad (4.30)$$

$$\frac{\Delta\varepsilon_e}{2} = \sigma'_f (2N)^b \quad (4.31)$$

Total strain amplitude of both elastic and plastic amplitude can be written

$$\frac{\Delta\varepsilon}{2} = \sigma'_f (2N)^b + \varepsilon_f (2N)^c \quad (4.32)$$

Cyclic fatigue ductility exponent and cyclic fatigue ductility coefficient are a parameters used find fatigue life in LCF. These parameters are temperature-dependent properties of the material. A below table and graph shows change of these two parameters with temperature taken from experimental data.

Table 4. 1 Cyclic ductility exponent and cyclic ductility coefficient at different temperature of 8.72Cr-0.9Mo steel (experimental data) [39]

| <b>Temperature in K</b> | <b>Cyclic ductility exponent</b> | <b>Cyclic ductility coefficient</b> |
|-------------------------|----------------------------------|-------------------------------------|
| 873                     | -0.96                            | 4.46                                |
| 823                     | -0.77                            | 1.34                                |
| 773                     | -0.67                            | 0.66                                |
| 673                     | -0.36                            | -3.54                               |

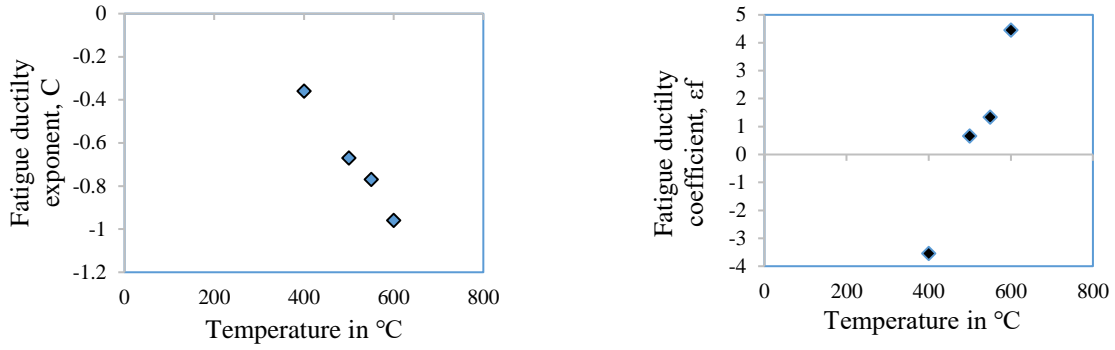


Figure 4. 17 Plot of cyclic ductility exponent and cyclic ductility coefficient at different temperature of 8.72Cr-0.9Mo steel [39]

For low cycle fatigue in plastic range, the number of cycle to failure can be calculated by Coffin and Manson relation

$$N_{f,LCF} = \frac{1}{2} \left( \frac{\Delta \epsilon_p}{2 \epsilon_f'} \right)^{1/c} \quad (4.33)$$

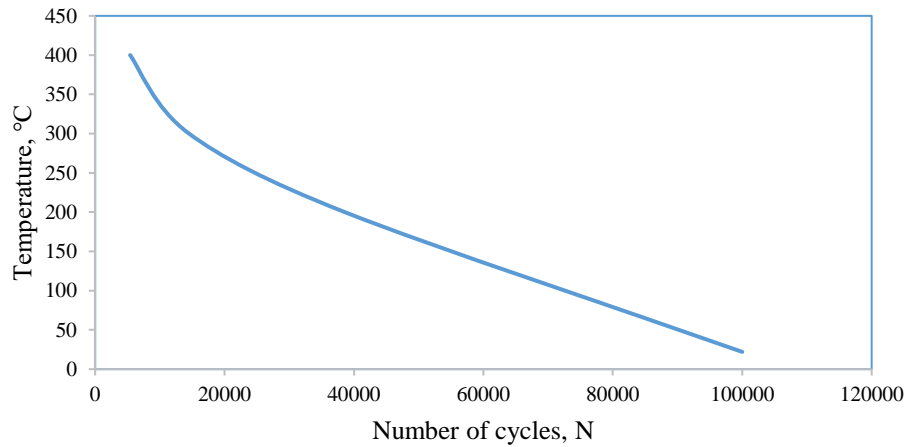


Figure 4. 18 Response of the 9Cr-1Mo steel to temperature in number of cycles

Where  $\Delta \epsilon_p$  plastic strain amplitude,  $\epsilon_f'$  fatigue ductility coefficient and  $c$  is the fatigue ductility exponent. Here there is no ratcheting since the strain resulting from cyclic stressing is small, so the failure is the result of low cycle fatigue (LCF) by constant strain amplitude because the stressing load, in this case, is only tensile as it was discussed in previous topic.

The following two graph shows, the effect of crack size on number of cycles and response of number of reversal to failure to strain amplitude change using Manson-Coffin equation.

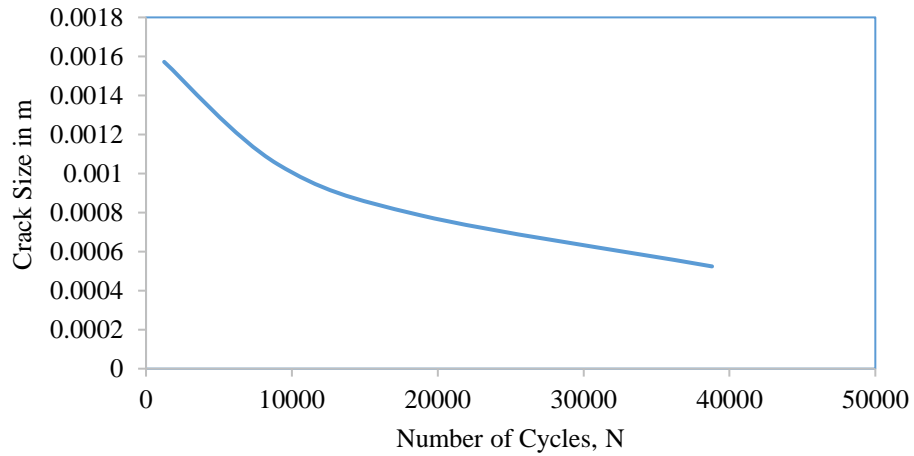


Figure 4. 19 Effect of crack size on number of cycles

According to Manson-Coffin, fatigue life not only depends on crack size it also depends on strain amplitude. The graph below shows the relationship between strain amplitude and number of reversal to failure.

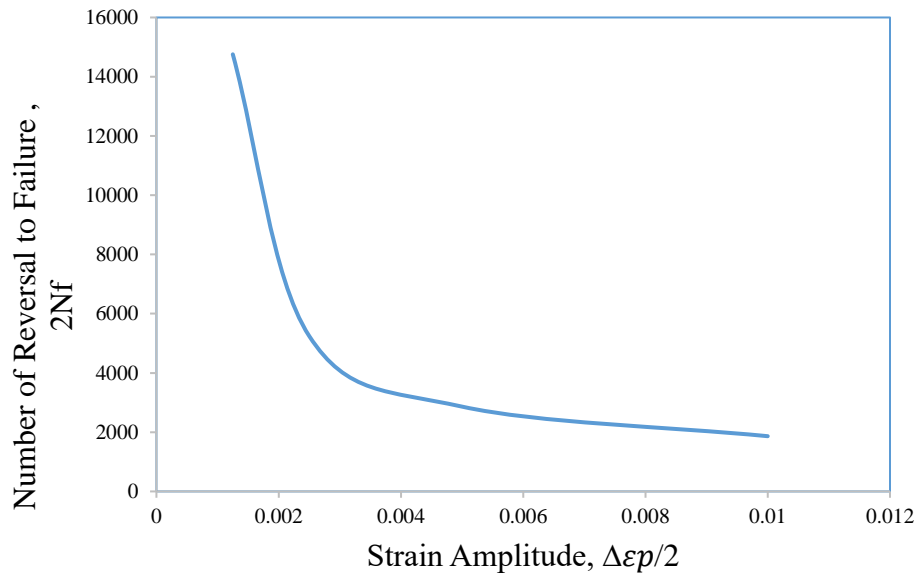


Figure 4. 20 Strain amplitude versus number of reversal to failure



#### 4.4.2 J-Integral Approach for Large Plastic Strain

Crack extension occurs when material at the crack tip exceeds its fracture strain due to continued strain cycling. Fatigue damage continuously accumulated within the plastic zone during cycling. Fatigue crack propagation by Paris is limited to linear-elastic deformation range when it used stress intensity factor in place of J-integral. But, it can be extended fracture mechanics concepts from linear-elastic to behavior to elastic-plastic behavior by using J-integral approach. For low cycle fatigue (LCF), fatigue crack propagation plastic deformation at the crack tip is dominant. The assumption taken here is edge crack, where crack grows into material subjected to uniform plastic strain field.

Fatigue crack growth rate (FCGR) can be expressed by elastic-plastic components of  $\Delta J$  integral by power law. J-integral is the rate at which energy is transformed as a material undergoes fracture and has units of energy-per-unit area. The energy release rate is central to the field of fracture mechanics when solving problems and estimating material properties related to fracture and fatigue. The fatigue crack growth rate is calculated as a function of J-integral range as follows

$$\frac{da}{dN} = C_f (\Delta J)^{m_f} \quad (4.34)$$

$C_f$  and  $m_f$  are a material constant and it is assumed that in this study  $R=0$  and J-integral range  $\Delta J_{el}$  is calculated as equation (34) if only mode I is considered.

$$\Delta J_{el} = \frac{K_{max}^2}{E^*} \quad (4.35)$$

$K_{max}$  is the maximum stress intensity factor and the analysis is strain-based approach calculated as follow

$$E^* = \frac{E}{1-\nu^2} \quad (4.36)$$

The elastoplastic J-integral range  $\Delta J_{ep}$  is obtained from  $\Delta J_{el}$  using a plastic correction factor of  $f_{ep}$

$$\Delta J_{ep} = f_{ep} \times \Delta J_{el} \quad (4.37)$$

$$f_{ep} = \frac{\sigma_{ref}^3}{2\sigma_y^2 E \epsilon_{ref}} + \frac{E \epsilon_{ref}}{\sigma_{ref}} \quad (4.38)$$

$\sigma_{ref}$  is the reference stress calculated at the maximum load of the cycle. Here the J-integral is in plastic range, so that cyclic J-integral equal to elastoplastic cyclic J-integral. The dependence of crack growth rate on energy release during plastic deformation graphically shown in figure (20) below by taking the material constants,  $C_f=3.05 \times 10^{-5}$  and  $m_f=1.31$ .

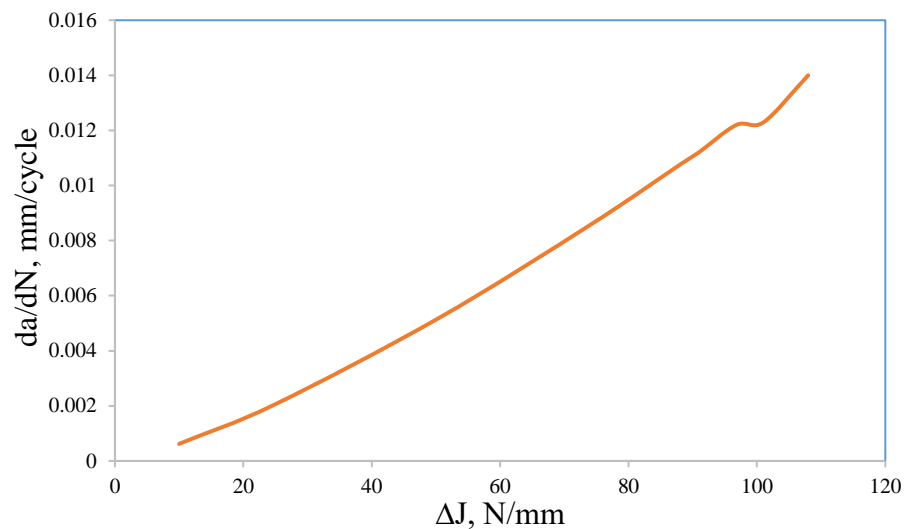


Figure 4. 21 Crack propagation rate versus cyclic J-integral using analytical approach

#### 4.5 Finite Element Method Simulation

The finite element method is the most widely used method for solving problems of engineering and mathematical models. It is a numerical technique used to perform finite element analysis of any given physical phenomenon. Today, product simulation is often being performed by engineering groups using niche simulation tools from different vendors to simulate various design attributes. The use of multiple vendor software products creates inefficiencies and increases costs. FEM delivers a scalable suite of unified analysis products that allow all users, regardless of their simulation expertise or domain focus, to collaborate and seamlessly share simulation data and approved methods without loss of information fidelity.

The ABAQUS/CAE is FEA product suite offers powerful and complete solutions for both routine and sophisticated engineering problems covering a vast spectrum of engineering applications. In the automotive industry, engineering workgroups are able to consider full vehicle loads, dynamic vibration, multibody systems, impact/crash, nonlinear static, thermal coupling, and acoustic-structural coupling using a common model data structure and integrated solver technology. Best-in-class companies are taking advantage of ABAQUS FEA to consolidate their processes and tools, reduce costs and inefficiencies, and gain a competitive advantage.

#### **4.5.1 Procedures**

ABAQUS standard/explicit used in this study. There a number of steps should be followed to get the final result from the software

1. “*Part module*” is a module where the model of the part is created.
2. There should be an input data like material properties, material properties given in “*property module*”.
3. In “*assemble module*” here if the analysis have multiple parts, it used to assemble independent parts. Creating mesh on part or on instance selected in this module.
4. The second is “*step module*” in this module it should have given the correct time period and increment size. And also “*field output*” and “*history output*” are a sub-option of step module where wanted outputs are selected.
5. The other important module is “*interaction module*” it is where the seam and crack is generated. Here “*contour integral*” is used.
6. “*Load module*” in this module load, boundary condition and predefined field set as per requirements.
7. “*Mesh module*” is where the appropriate mesh type selected and mesh size is fixed.
8. The last module used during analysis is “*job module*” it is where the input data submitted for solver.

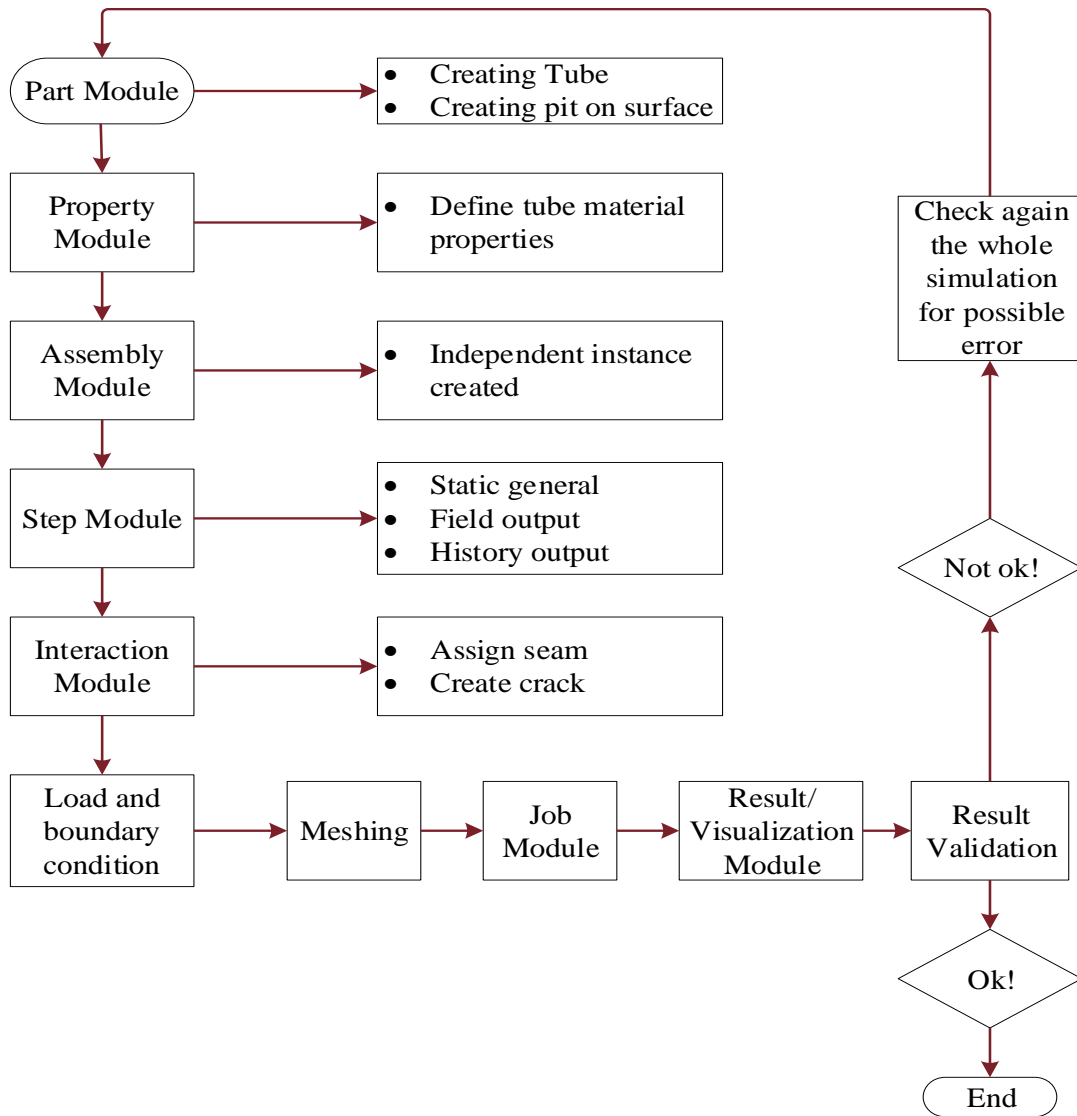


Figure 4. 22 Flow chart shows the procedure in finite element method

#### 4.5.2 Creating Part in ABAQUS

ABAQUS CAE with standard/Explicit a special purpose finite element analyzer that employs explicit integration scheme to solve highly nonlinear systems with many complexity and transient used. Doing analysis on the whole part of the model difficult, because it takes large memory during computation of the problem. So that only section of the part have taken for software analysis. As it's shown on the figure left side it is the full model of the component and the one at right side shows the section part of the component. This do not have any effects

on the expect result for the software rather it reduce the memory space and it reduce the time consumed during analysis for the solver.

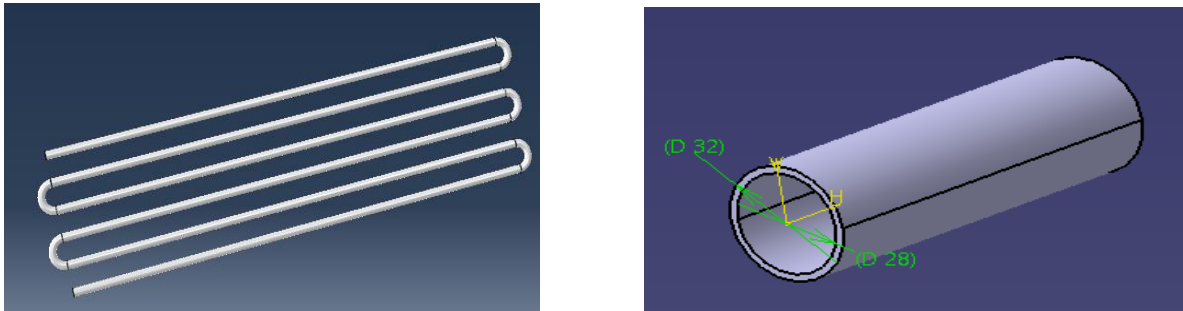


Figure 4. 23 Abaqus model of boiler heater tube

#### 4.5.3 Mesh Type

Mesh is a network that is formed of cells and points. It can have almost any shape in any size and is used to solve partial differential equations. Each cell of the mesh represents an individual solution of the equation which, when combined for the whole network, results in a solution for the entire mesh. A 14698 3-nodes linear triangular (S3) shell element mesh type with approximate global size of 1mm used, it is compatible for crack propagation analysis under large plastic deformation at crack tip. Here no need of checking mesh sensitivity because there is no solid to solid contact in this case.

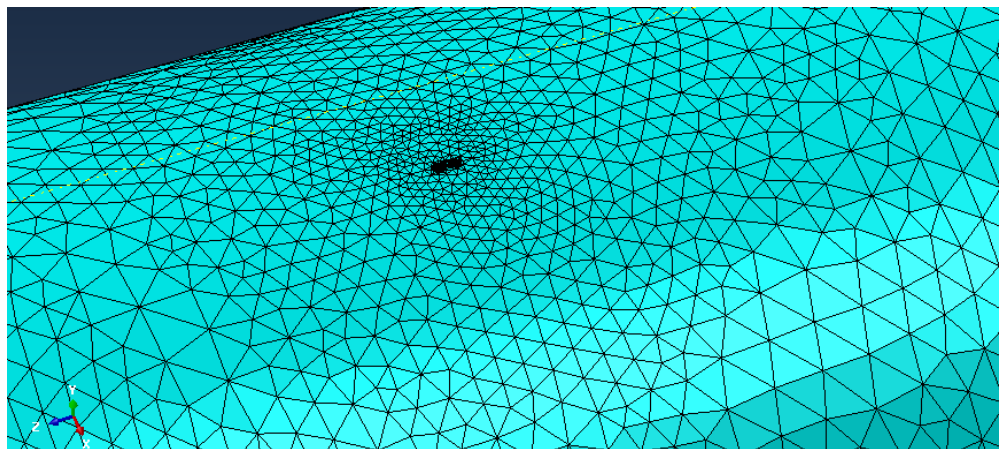


Figure 4. 24 Triangular mesh surface of the tube

#### 4.5.4 Simulation Result

The term simulation is a process of creating a model of an existing or proposed system in order to identify and understand those factors which control the system and predict the behavior of the system. The following simulations are a results from ABAQUS software. The simulations shows stress distribution in the model or at crack tip, plastic strain at crack tip and plastic strain energy density at crack tip. The boundary condition taken as the inner tube surface heated by hot gas or flame and outer surface kept at steam temperature or operating steam temperature. As an input file the tube allowed to expand in circumfrential and longitudinal direction only. In radial direction taken assumed to be zero. The figure below shows the result/simulation from ABAQUS software of Von-Mises stress developed at 500°C, with a maximum 895Mpa and minimum of 25Ma.

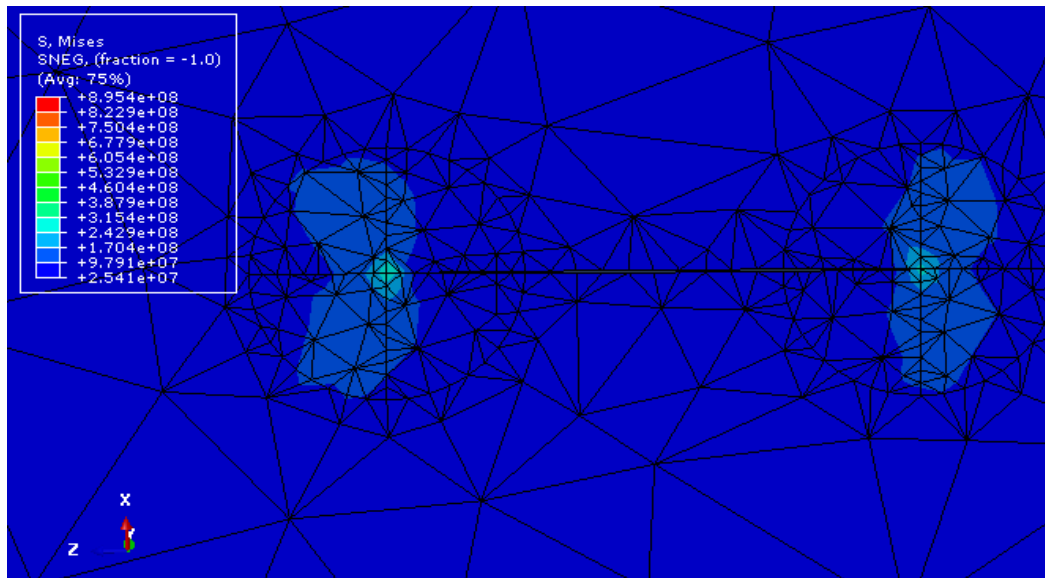


Figure 4. 25 Stress distribution around crack tip (Von-Mises stress)

The simulation below shows the result of strain at and around the crack tip having the maximum value of  $6.077 \times 10^{-3}$ . From the simulation, it is seen that the maximum value is at crack tip, it is highlighted and indicated on contour. The result is cyclic plastic strain (plastic deformation) that results from cyclic thermal stress. This plastic deformation at crack tip cause separation and crack will propagate.



Figure 4. 26 Strain at the crack tip under thermal stress

Strain energy density describes the relationship between the amount of energy employed to deform a volume unit of a solid and imposed strain or it nothing but the area under the stress-strain curve in plastic range. Plastic strain energy density (PENER) shown in the following simulation, in ABAQUS PENER is used to calculate J-integral value. Using the maximum value from the result of software having the value of  $6.89 \times 10^6 \text{ j/m}^3$  or  $6.89 \times 10^6 \text{ N/m}^2$ . Cyclic J-integral is calculated to be  $35.43 \text{ N/mm}$  or  $35.43 \text{ J/mm}^2$  from the below simulation result at  $500^\circ\text{C}$  of thermal load.

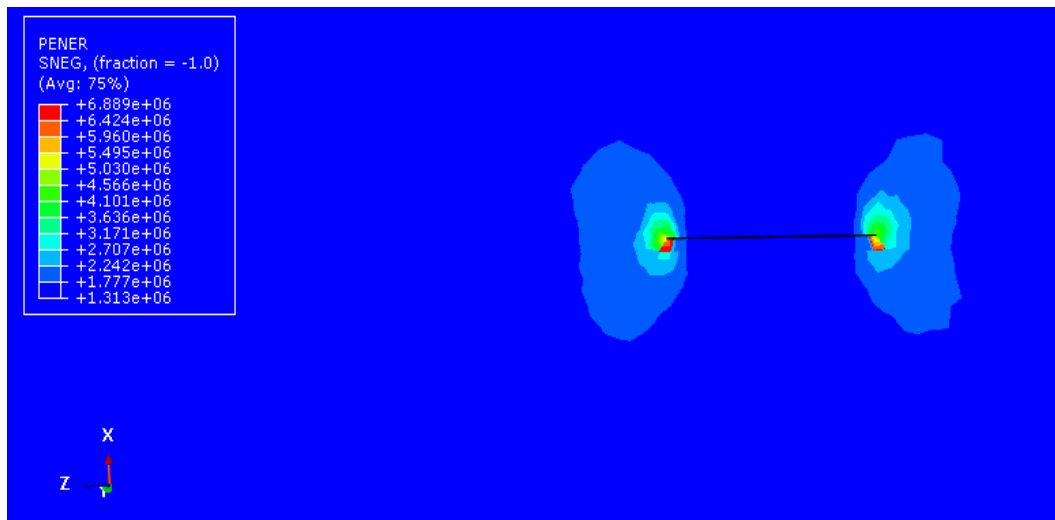


Figure 4. 27 Plastic strain energy density (PENER)

## Chapter

# 5

## Results and Discussion

Whenever the material is under a load, it will respond to the applied load, this applied load develops stress on the material and it might deform elastically or plastically. If this load is cyclically applied, it causes what is so-called fatigue. The cyclic load reduces the intended life of the components. Nowadays 8.72Cr-0.9Mo steel is mostly used as material in power generating power plants and reactors. Corrosion is also a parameter which reduces the life of the materials, especially when combined with cyclic loading.

In section (4.3.2) corrosion rate changes with temperature. The result shows that changes in temperature have a great influence on the rate of corrosion.

Temperature influences the rate of corrosion by increasing kinetic energy at the molecular level. This facilitates the collision between particles which can alter the reaction rate. Especially, above 250°C there is a significant change in volumetric pit growth rate as shown in figure (30) below. Activation energy does not change with temperature significantly, rather it is affected by the presence of inhibitors and catalysts.



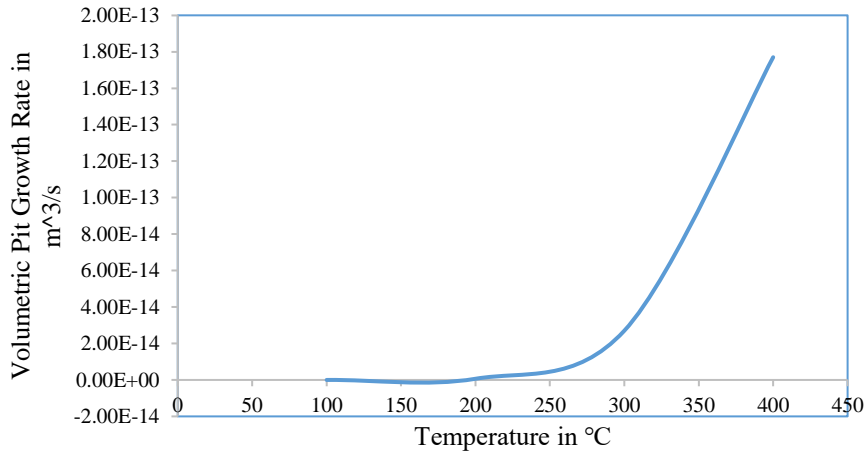


Figure 5. 1 Volumetric pit growth rate response to temperature change

Temperature is not only affect the rate corrosion but also alter the properties of the steel metal. The properties like young’s modulus, thermal expansion coefficient, ductility coefficient, ductility exponent and others are significantly change with temperature change. These change in material properties directly related to fatigue life or service life of the component in both during crack initiation and crack propagation stages.

Pit to crack transition happen when pit reach critical value  $a_{cr}$  and transition depends on different factors like volumetric pit growth rate, stress intensity factor, and cyclic stress. Volumetric pit growth rate is the main factor that affect this transition since the pit is initiated by the corrosion. A large volumetric pit growth rate reduce the cyclic life to initiate crack initiation and vice versa.

The stage after crack initiation is crack propagation stage where the crack propagate in bulk. At this stage, crack propagate transgranular up to failure of the component. Crack propagation dominated by irreversible large plastic deformation at crack and plastic zone around crack tip. Since the component is subjected to cyclic thermal stress, which induces tensile stress, mode I is dominant than other types of fatigue failure modes.

In low cyclic fatigue, the cycle to failure not exceed  $10^5$  or is below this value of cycles. For crack initiation state, it is used that volumetric pit growth rate up to the critical value of pit crack transition. Cyclic fatigue life is calculated using strain-based approach for crack propagation stage.

Strain based approach analysis using Manson-Coffin equation depends on the cyclic strain, ductility coefficient, and exponent. Ductility coefficient and exponent are sensitive to temperature change and the value is taken from other literature result respective to temperature. 8.72Cr-0.9Mo steel ductility coefficient and ductility exponent increase with the increase of temperature in magnitude.

The comparison between other literature (experimental data) and analytical have a good agreement. Analytical result found taking the temperature of the surface of part 500°C and calculating the strain amplitude. Using Manson-Coffin expression the number of reversal to failure is calculated. The result from this expression have good approximation with other literature data. Figure (27) shows the comparison among analytical, finite element method and other literature.

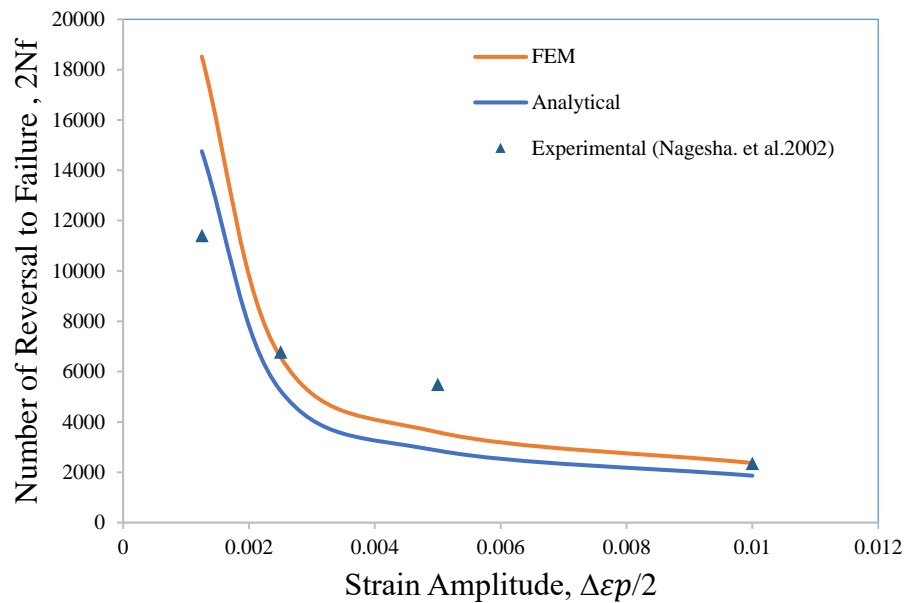


Figure 5. 2 Comparison between analytical, FEM and other literature (experimental result) using strain amplitude versus number of reversal to failure at 500°C (773K)

From the results, it is observed that at large strain amplitude have low fatigue life. The result computed by taking fatigue ductility coefficient  $\epsilon_f = 0.66$  and fatigue ductility exponent  $C = -0.67$  at 500°C or 773k from experimental data.

Corrosion pit reduce the fatigue life with a significant value. In Manson-Coffin expression the fatigue life depends on the fatigue ductility exponent and fatigue ductility coefficient. The

presence of pit and high temperature increase these values. The smaller the value of fatigue ductility coefficient and fatigue ductility exponent, large number of fatigue life and vice versa. The graph below shows the comparison between the fatigue life of boiler heat tube with corrosion pit and without corrosion pit. The result indicate there is a large difference between the two. However, the results have close result to each other for large cyclic strain amplitude. At large cyclic strain, the effect of pit is no more produce effect as shown below. When the fatigue occurs under corrosion pit, the fatigue cycles limited below 20,000 cycles at minimum strain amplitude. But without corrosion pit this number can increased to upto 200,000 cycles at minimum strain amplitude.

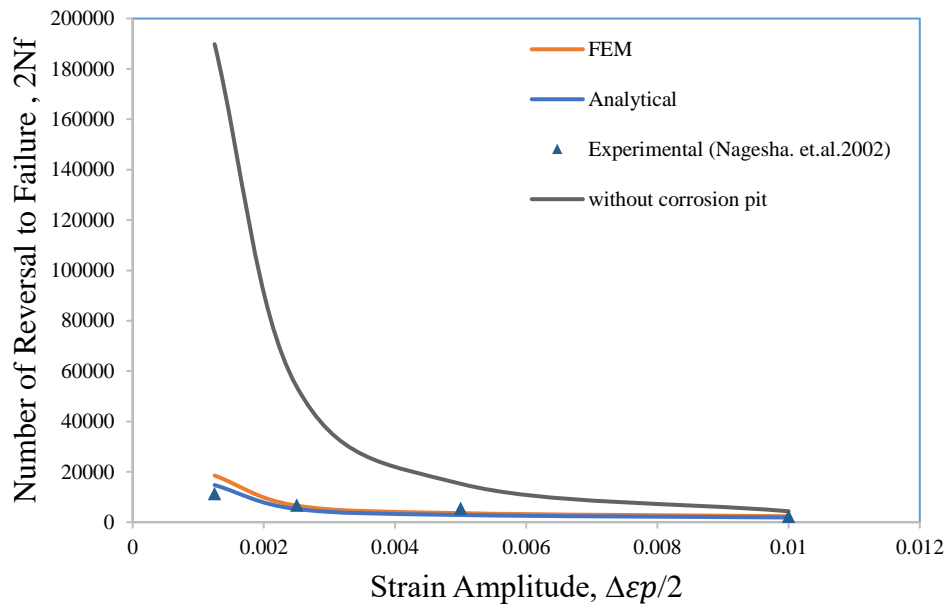


Figure 5. 3 Comparison between fatigue with corrosion pit and without corrosion pit

The result from analytical at this temperature thermal strain of  $6.6 \times 10^{-3}$  which is almost equal to finite element result  $6.06 \times 10^{-3}$ . And also thermal stress induced due to thermal load analytically predicted to 906Mpa and finite element result gives 895Mpa which close value to analytical result.

The result shows J-integral and crack growth rate have a direct proportionality. The graph below compare analytical result which is calculated, finite element and experimental data taken from the literature [37]. Analytical model have very nice agreement with experimental data.

From the graph, it is clearly observed that large crack growth rate means it release large energy during plastically deformation of crack tip.

The cyclic J-integral ( $\Delta J$ ) finite element method (FEM) is estimated to 35.43N/mm or 35.43J/mm<sup>2</sup> at 500°C and from analytical approach is calculated to 33.4N/mm at the thermal load. These two results have close value and only having deviation of below 10% from each other.

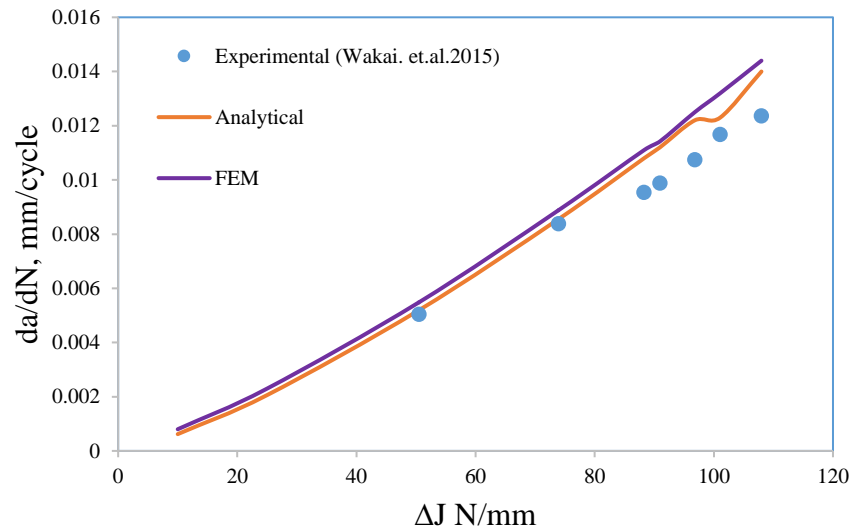


Figure 5. 4 Comparison of analytical, FEM and other literature (experimental data) of crack growth rate versus cyclic J-integral

The graph below shows the cycles takes to initiate crack and crack propagation at different crack length or size. This describes the length of crack at a number of cycle. It generally indicates that crack growth in length as number of cycle increases. At the beginning crack initiation has a low growth rate but when it starts to propagate it growth fast rate.

During crack initiation stage is believed that it takes more number of cycles than crack propagation stage but, on the result below it takes a cycles not less than crack initiation stage. This can be interpreted as the presence of corrosion pit significantly reduce the number of cycles that take to initiate the crack. Here it implies corrosion reduce intended service life of this component when compared to the component that service under a media of non-corrosive

environment. The graph shows simultaneously crack initiation and crack propagation stage. However, this not to say the two phenomenon are happened at the same time.

At the beginning pit growth intergranular along grain boundaries, when pit reach at critical value (pit to crack transition value), it changed to grow transgranular across grain. During this stage, crack grow in bulk.

The result shows, fatigue condition is within range of the low cycle fatigue (below  $10^5$  cycles). Crack propagation (crack size versus number of cycles) found have very close value with experimental result. This graph shows the comparison of analytical, FEM and experimental data (other literature). The results have good agreement to each other with small deviation in acceptable range.

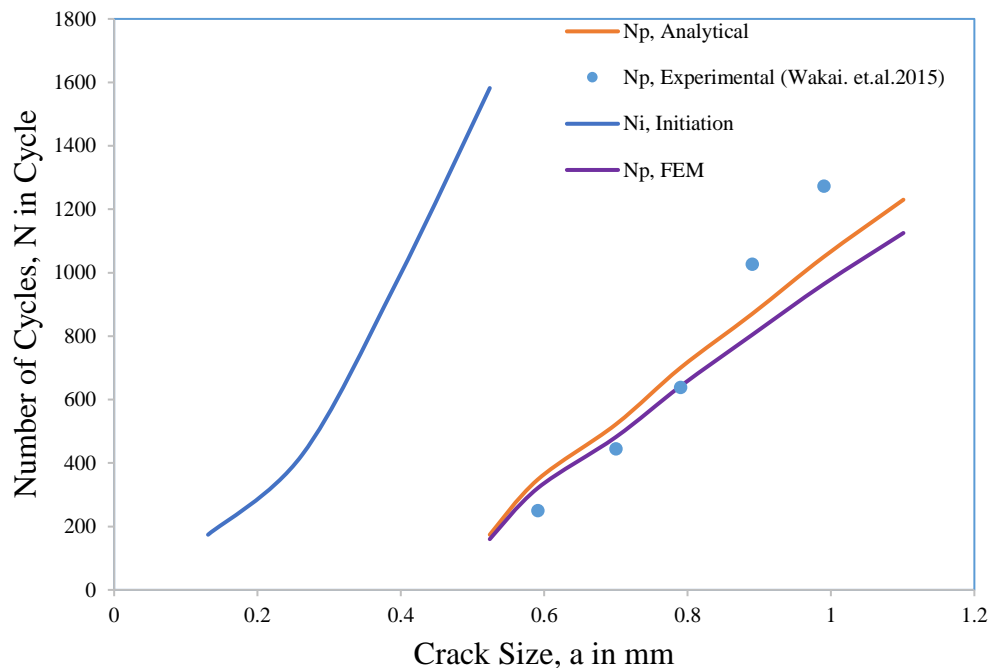


Figure 5. 5 Comparison between analytical, FEM and other literature (experimental data), crack initiation and crack propagation results

The total life the tube is the summation of number of cycles to take crack initiation  $N_{in}$  and number cycles takes during propagation stage  $N_p$ . As discussed above, crack initiation was

calculated from volumetric pit growth rate up to the critical value of pit, when it reaches critical value crack will be initiated. Then after crack propagation starts from initiation to final failure of the component. The two result varies with load value, for example, if the tube operating under a temperature of 500°C the crack initiation and crack propagation have a less number of cycles than 400°C thermal load.

The results found from both analytical approach and finite element method (FEM) have a deviation below 10% from other literature (experimental data). Thus, those results are valid, since the values are in acceptable range.

## Chapter

# 6

## Conclusion and Recommendation

### 6.1 Conclusion

This study addressed a fatigue phenomenon of 8.72Cr-0.9Mo steel boiler tube under cyclic thermal loading and corrosion pitting. Analytical and finite element method (FEM) are two methods, and strain-based approach (i.e. low cycle fatigue), used during analysis. Corrosion rate in pit growth rate up to crack initiation and crack propagation were the main concern of this study.

The crack initiated by pit growth on the surface of the boiler. Pit growth rate can be influenced by temperature on surface of the tube. Temperature is most influencing factor. It also affect the material properties, like young's modulus, tensile strength, fracture toughness, and other mechanical properties which reduce the fatigue strength of the boiler. The overall change in material have a negative effect on fatigue life of the component. That means it significantly affect fatigue life.

Crack propagation rate was estimated using energy release rate in both analytical and finite element approaches. Cyclic J-integral (energy release rate) method with Paris law was used and the result have good approximation with other literature (experimental data). As energy release rate increase, crack propagation rate increases. In normal fatigue analysis of the material, crack initiation takes longer time than crack propagation stage. However, here due to presence of corrosion crack initiation takes almost equal life cycles when compared to crack propagation stage in this study.

In general, the fatigue life of the boiler tube under thermal load is not only by the cyclic thermal loading, it is also altered by the change in material properties of the steel used as well as it depends on the existence of corrosion.

As a limitations during this research, there are a number of difficulties to conduct experimental test due to a shortage of laboratory facilities. Not only laboratory equipment, conducting test on fatigue test is somewhat tough and tedious because of the test should conduct several time which consume both time and resources. So that this work only limited to only analytical and finite element study only. To check whether the result found correct or not it compared with experimental data of other literature.



## **6.2 Recommendation**

During this study there are areas where further work is needed. The first area is there is no experimental investigation of pit growing under thermal cyclic loading conditions for modified 9Cr-1Mo steel and thus the study analytically predicts the pit growth rate. The assumption taken here is the corrosion media is water (moisture) and the oxygen the corrosion to happen or occur.

The second area is tube thickness is assumed to be thin and avoiding the thermal radial stress to be insignificant because of small deformation radially. But in for tube which have large wall thickness, it might have a significant effect since it deforms in radial direction and it should have been taken into consideration.

Additionally in this research only axial direction cracking is considered, so one may further study by adding crack along circumference and also one may study multiple pits that may cause cracking by growing in coalescence in short cycles. And also oxides debris crack closure effect is not considered during the study.

## References

1. Katarina M. Dragi S, and Ivana V. *Determination of Fracture Mechanics Parameters Structural Components with Surface Crack Under Thermomechanical Loads. Scientific Technical Review, 2016, Vol.66, No.3, pp.27-33*
2. Tu T, Zhang C. *Fatigue crack initiation mechanisms. Reference Module in Materials Science and Materials Engineering.*
3. *ASM Handbook, Volume 13, "Corrosion", ISBN 0-87170-007-7, ASM International, 1987*
4. Xin Q. *Durability and reliability in diesel engine system design. Diesel Engine System Design. 2013:113-202.*
5. Casey T, Shane T. *Failure analysis of cracked boiler tube*
6. Kondo Y. *Prediction of fatigue crack initiation life based on pit growth. Corrosion. 1989 Jan;45(1):7-11.*
7. Miguel L. and Infante B. Béjar M. *Corrosion-fatigue testing on steel grades with different heat and surface treatments used in rock-drilling applications. 2012*
8. Gangloff P. *Environmental cracking-corrosion fatigue. ASTM manual series mnl. 1995:253-71.*
9. Jones R, editor. *Stress-Corrosion Cracking, Materials performance, and evaluation. ASM International; 2017.*
10. Ramsamooj V, Shugar A. *Modeling of corrosion fatigue in metals in an aggressive environment. International Journal of Fatigue. 2001 Jan 1;23:301-9.*
11. Acuña N, González A, Dzib R, Rivas A. *Early corrosion fatigue damage on stainless steels exposed to tropical seawater: a contribution from sensitive electrochemical techniques. In Applied fracture mechanics 2012 Dec 12. IntechOpen.*
12. Kumari A, Das S, Srivastava K. *Modeling fireside corrosion rate in a coal-fired boiler using adaptive neural network formalism. Portugaliae Electrochimica Acta. 2016 Jan;34(1):23-38.*
13. McEvily A, Wei R. *Fracture mechanics and corrosion fatigue. Connecticut Univ Storrs Dept of Metallurgy; Feb 1972*
14. Boyer H, editor. *Atlas of fatigue curves. Asm International; 1985 Dec 31.*

15. Seifert H, Ritter S, Leber H. Corrosion fatigue crack growth behavior of austenitic stainless steels under light water reactor conditions. *Corrosion Science*. 2012 Feb 1;55:61-75.
16. Khaleel H, Ateeq A, Ali A. The Effect of Temperature and Inhibitor on Corrosion of Carbon Steel in Acid Solution under Static Study. *International Journal of Applied Engineering Research*. 2018;13(6):3638-47.
17. Rahman M, Purbolaksono J, Ahmad J. Root cause failure analysis of a division wall superheater tube of a coal-fired power station. *Engineering Failure Analysis*. 2010;6(17):1490-4.
18. Para S. *Corrosion-fatigue cracking behavior of weld clad tubes*. 2004
19. Ahmad J, Purbolaksono J, Beng LC. Thermal fatigue and corrosion fatigue in heat recovery area wall side tubes. *Engineering Failure Analysis*. 2010 Jan 1;17(1):334-43.
20. Jinu G, Sathiya P, Ravichandran G, Rathinam A. Comparison of thermal fatigue behavior of ASTM A 213-grade T-92 base and weld tubes. *Journal of mechanical science and technology*. 2010 May 1;24(5):1067-76.
21. Agrawal R, Uddanwadiker R, Padole P. Low cycle fatigue life prediction. *Int J Emer Eng Res Technol*. 2014 Jul;2(4):5-15.
22. Milella P. *Fatigue and corrosion in metals*. Springer Science & Business Media, 2013.
23. Tolcha M, Altenbach H, Tibba G. Modeling fatigue crack and spalling for rolling die under hot milling. *Fatigue & Fracture of Engineering Materials & Structures*.
24. Glinka G. Calculation of inelastic notch-tip strain-stress histories under cyclic loading. *Engineering Fracture Mechanics*. 1985 Jan 1;22(5):839-54.
25. Živica V. Significance and influence of the ambient temperature as a rate factor of steel reinforcement corrosion. *Bulletin of Materials Science*. 2002 Oct 1;25(5):375-9.
26. Xuejun H. *Experimental and Modelling Studies of Pit-to-Crack Transition under Corrosion Fatigue Conditions*
27. Cerit M, Genel K, and Eksi S. "Numerical investigation on stress concentration of corrosion pit," *Eng. Fail. Anal.*, vol. 16, no. 7, pp. 2467–2472, 2009.
28. Haddad H, Topper H, and Smith N. "Prediction of non-propagating cracks," *Eng. Fract. Mech.*, vol. 11, no. 3, pp. 573–584, Jan. 1979

29. Kaisand R and Mowbray, D. F. 'Relationships between low cycle fatigue and crack growth rate properties' *J of Testing and Evaluation* 7 No 5 (1979) pp 270--280L.
30. ASM International, *elements of metallurgy and engineering alloys*.
31. Ishihara S, Saka S, Nan Z, Goshima T, and Sunada S. "Prediction of Corrosion-Fatigue Lives of Aluminum Alloy on the Basis of Corrosion Pit Growth Law," *Fatigue and Fracture of Engineering Materials and Structures*, Vol. 29, No. 6, 2006, pp. 472–480.
32. Mowbray F. 'Relationships between low cycle fatigue and crack growth rate properties' *J of Testing and Evaluation* 7 No 5 (1979) pp 270—280
33. McEvily J. 1974. "Phenomenological and Microstructural Aspects of Fatigue". Presented at the Third International Conference on the Strength of Metals and Alloys, Cambridge, England; published by The Institute and The Iron and Steel Institutes, Publication, W36, PP. 204-213.
34. Collipriest J. An experimentalist's view of the surface flaw problem. Paper from "The Surface Crack- Physical Problems and Computational Solutions", ASME, New York. 1972, 43-61.. 1972.
35. Frost E, Pook P, Denton K. A fracture mechanics analysis of fatigue crack growth data for various materials. *Engineering Fracture Mechanics*. 1971 Aug 1;3(2):109-26.
36. Dowling E, Begley A. Fatigue crack growth during gross plasticity and the J-integral. *mechanics of crack growth* 1976 Jan. ASTM International.
37. Wang W, Hsu T. Fatigue crack growth rate of metal by plastic energy damage accumulation theory. *Journal of engineering mechanics*. 1994 Apr;120(4):776-95.
38. ASTM E. 02. Standard test method for determination of reference temperature, T<sub>0</sub>, for ferritic steels in the transition range. *Annual book of ASTM standards*. 1921;3:1068-84.
39. Choudhary K, Nagesha A, Bhanu K and Baldev R. *On The Fatigue Deformation and Damage in 9%Cr Ferritic Steels*
40. Xu C, Yao H, Dong X, Jiang K. Mechanism of high-temperature oxidation effects in fatigue crack propagation and fracture mode for FGH97 superalloy. *Rare Metals*. 2019 Jul 10;38(7):642-52.

41. Wakai T, Inoue O, Ando M, Kobayashi S. *Thermal fatigue crack growth tests and analyses of thick wall cylinder made of mod. 9Cr–1Mo steel. Nuclear Engineering and Design.* 2015 Dec 15;295:797-803
42. Chandravathi S, Laha K, Bhanu K, Mannan L. *Microstructure and tensile properties of modified 9Cr–1Mo steel (grade 91). Materials science and technology.* 2001 May 1;17(5):559-65.
43. Sikka K. *Development of modified 9 Cr-1 Mo steel for elevated-temperature service. Oak Ridge National Lab.;* 1983.
44. Nagesha A, Valsan M, Kannan R, Rao B, Mannan SL. *Influence of temperature on the low cycle fatigue behavior of a modified 9Cr-1Mo ferritic steel. International Journal of Fatigue.* 2002 Dec. 1;24(12): 1285-93
45. *Corrosionchemistry:*[https://chem.libretexts.org/Bookshelves/General\\_Chemistry/Map%3A\\_Chemistry](https://chem.libretexts.org/Bookshelves/General_Chemistry/Map%3A_Chemistry)
46. Dudziak T, Łukaszewicz M, Simms N, Nicholls J. *Analys of high-temperature steam oxidation of superheater steels used coal-fired boilers. Oxidation of Metals.* 2016 Feb 1;85(1-2):171-87.
47. Aris R. *Mathematical modeling techniques. Courier Corporation;* 1994.
48. Dym C, Ivey E, Stewart M. *Principles of mathematical modeling. American Journal of Physics.* 1980 Nov;48:994-5.

# Appendixes

## Appendix A

### Constants

**Table A-1**

Mechanical properties of 8.72Cr-0.9Mo steel

| Constants                     | Value            |
|-------------------------------|------------------|
| Young modulus E               | 200Gpa           |
| Yield strength $\sigma_y$     | 533Mpa           |
| Tensile strength              | 669Mpa           |
| Poison's ratio elastic range  | 0.3              |
| Poison's ratio plastic range  | 0.5              |
| Fracture Toughness            | 41Mpa $\sqrt{m}$ |
| Fatigue ductility exponent    | -0.67 at 500°C   |
| Fatigue ductility coefficient | 0.66 at 500°C    |

**Table A-2**

Physical properties of 8.72Cr-0.9Mo steel

|                    |                               |
|--------------------|-------------------------------|
| Molecular weight   | 55.84g/mol                    |
| Pitting current    | $200\mu A/cm^2$               |
| Valance            | 3                             |
| Faraday's constant | $9.65 \times 10^7 C/Kg - mol$ |
| Density            | $7800kg/m^3$                  |
| Activation energy  | 18.69kj/mol                   |
| Gas constant       | 8.314j/mol.k                  |

## Appendix B

### Tubes Wall Thickness and Outside Diameter

ASTM A213/ASME 8.72Cr-0.9Mo steel tubes wall thickness and tolerance

|            |                                    |               |
|------------|------------------------------------|---------------|
|            | Outside diameter, mm               | Tolerance, %  |
|            | $OD \leq 101.6, WT \leq 2.4$       | +40/-0        |
| Hot rolled | $OD \leq 101.6, 2.4 < WT \leq 3.8$ | +35/-0        |
|            | $OD \leq 101.6, 3.8 < WT \leq 4.6$ | +33/-0        |
|            | $OD \leq 101.6, WT > 4.6$          | +28/-0        |
|            | $OD > 101.6, 2.4 < WT \leq 3.8$    | +35/-0        |
|            | $OD > 101.6, 3.8 < WT \leq 4.6$    | +33/-0        |
|            | $OD > 101.6, WT > 4.6$             | +28/-0        |
|            | Outside Diameter, mm               | Tolerance , % |
| Cold Drawn | $OD \leq 38.1$                     | +20/-0        |
|            | $OD > 38.1$                        | +22/-0        |



ASTM A213/ASME 8.72Cr-0.9Mo Steel Tubes Outside Diameter and Tolerance

|            | Outside Diameter, mm      | Tolerance, mm |
|------------|---------------------------|---------------|
| Hot rolled | $OD \leq 101.6$           | +0.4/-0.8     |
|            | $101.6 < OD \leq 190.5$   | +0.4/-1.2     |
|            | $190.5 < OD \leq 228.6$   | +0.4/-1.6     |
|            | Outside Diameter, mm      | Tolerance, mm |
|            | $OD < 25.4$               | $\pm 0.10$    |
|            | $25.4 \leq OD \leq 38.1$  | $\pm 0.15$    |
|            | $38.1 < OD < 50.8$        | $\pm 0.20$    |
|            | $50.8 \leq OD < 63.5$     | $\pm 0.25$    |
|            | $63.5 \leq OD \leq 76.2$  | $\pm 0.30$    |
|            | $76.2 \leq OD \leq 101.6$ | $\pm 0.38$    |
|            | $101.6 < OD \leq 190.5$   | +0.38/-0.64   |
|            | $190.5 < OD \leq 228.6$   | +0.38/-1.14   |

## Appendix C

### Analytical approach additional calculation

From software result ABAQUS generate plastic strain energy density (PENER), but to find energy release rate or cyclic J-integral using the following relationship

$$\Delta J = 2\pi Y^2 a w$$

Here w is plastic strain energy density taken from simulation result, a is crack size and Y is geometric correction factor edge crack having the value of 1.25.

$$\Delta J = 2\pi(1.25)^2 \times 0.000524 \times 6.889 \times 10^6$$

$$\Delta J = 35.4 \times 10^3 \text{ N/m or}$$

$$\Delta J = 35.4 \text{ N/mm}$$

The above value is cyclic J-integral value at crack tip during plastic deformation.